AD 289 326

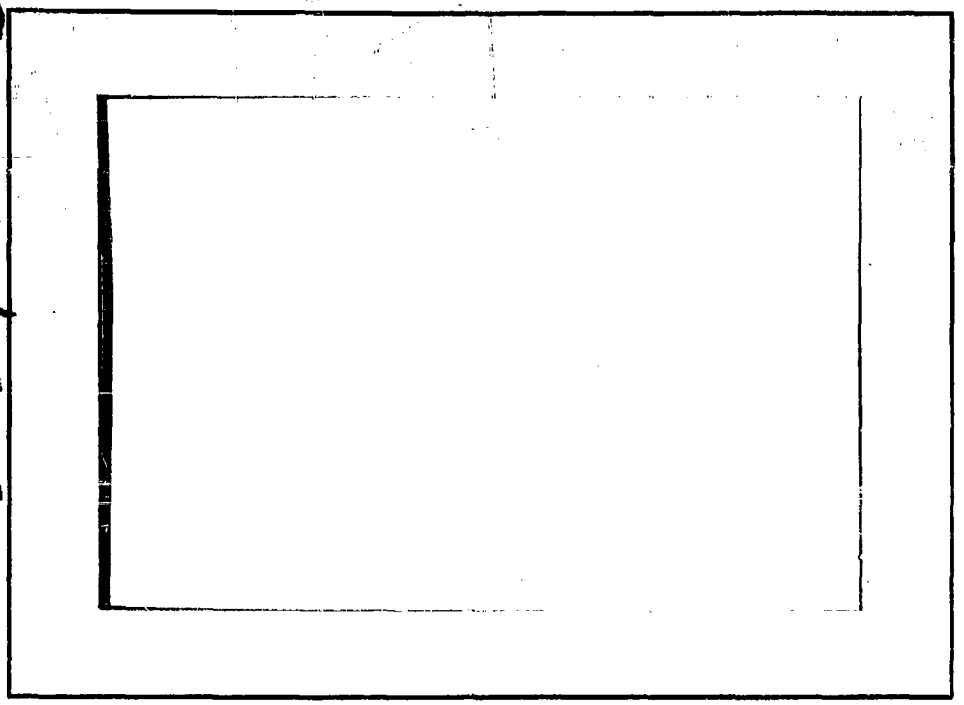

ATMOSPHERIC PHYSICS

School of Physics

UNIVERSITY OF MINNESOTA

TWO ATMOSPHERIC CONSTITUENTS

OZONE AND SMALL IONS

John L. Kroening

Technical Report AP-20

Atmospheric Physics Program

Navy Contract No. NONR 710(22)

September 1962

This paper was written in partial fulfillment of
the requirements for the degree of
Doctor of Philosophy

TABLE OF CONTENTS

ILLUSTRATIONS

Small Ions

TABLES

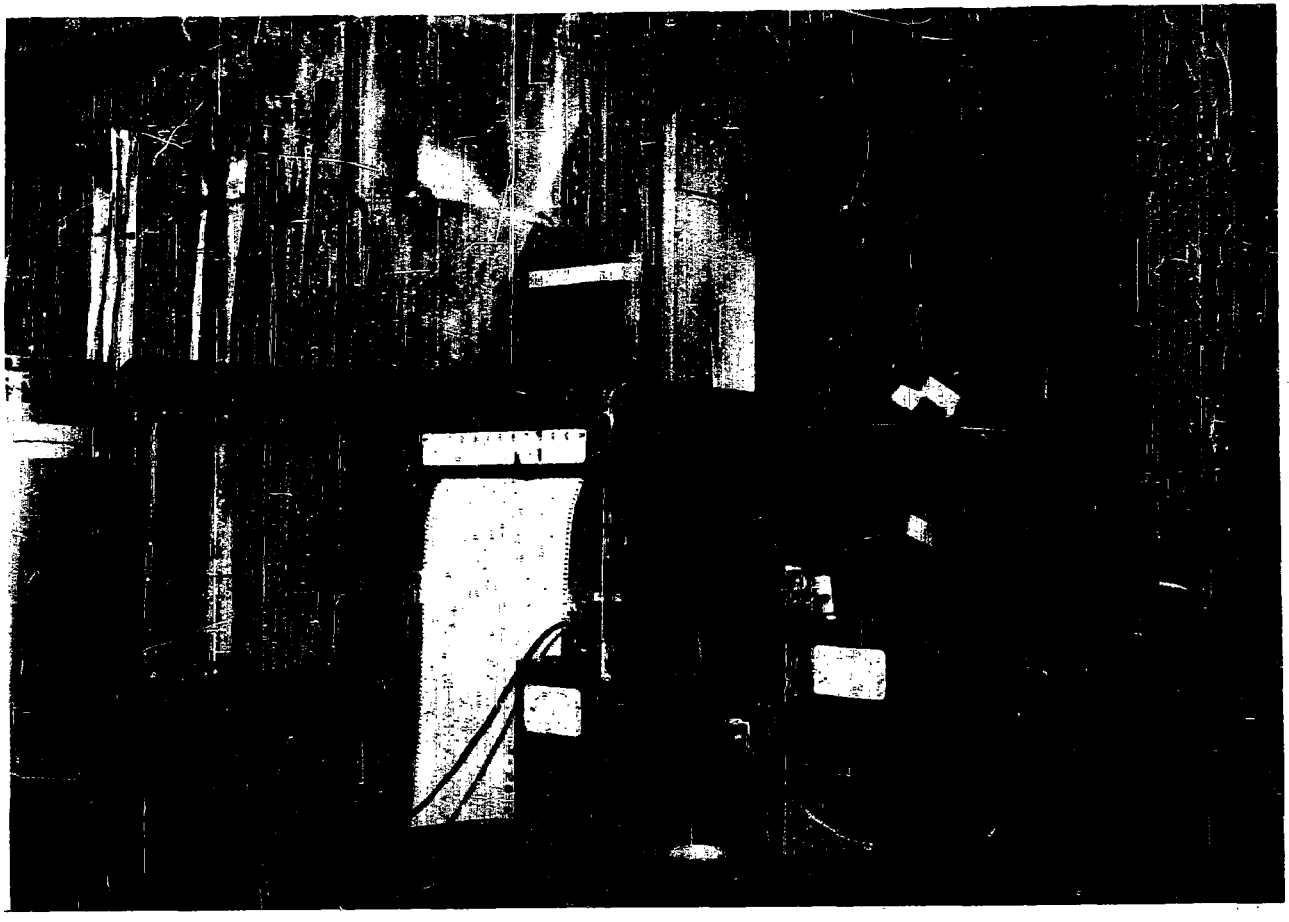

The ground level ozone monitor at the University of Minnesota Physics Building

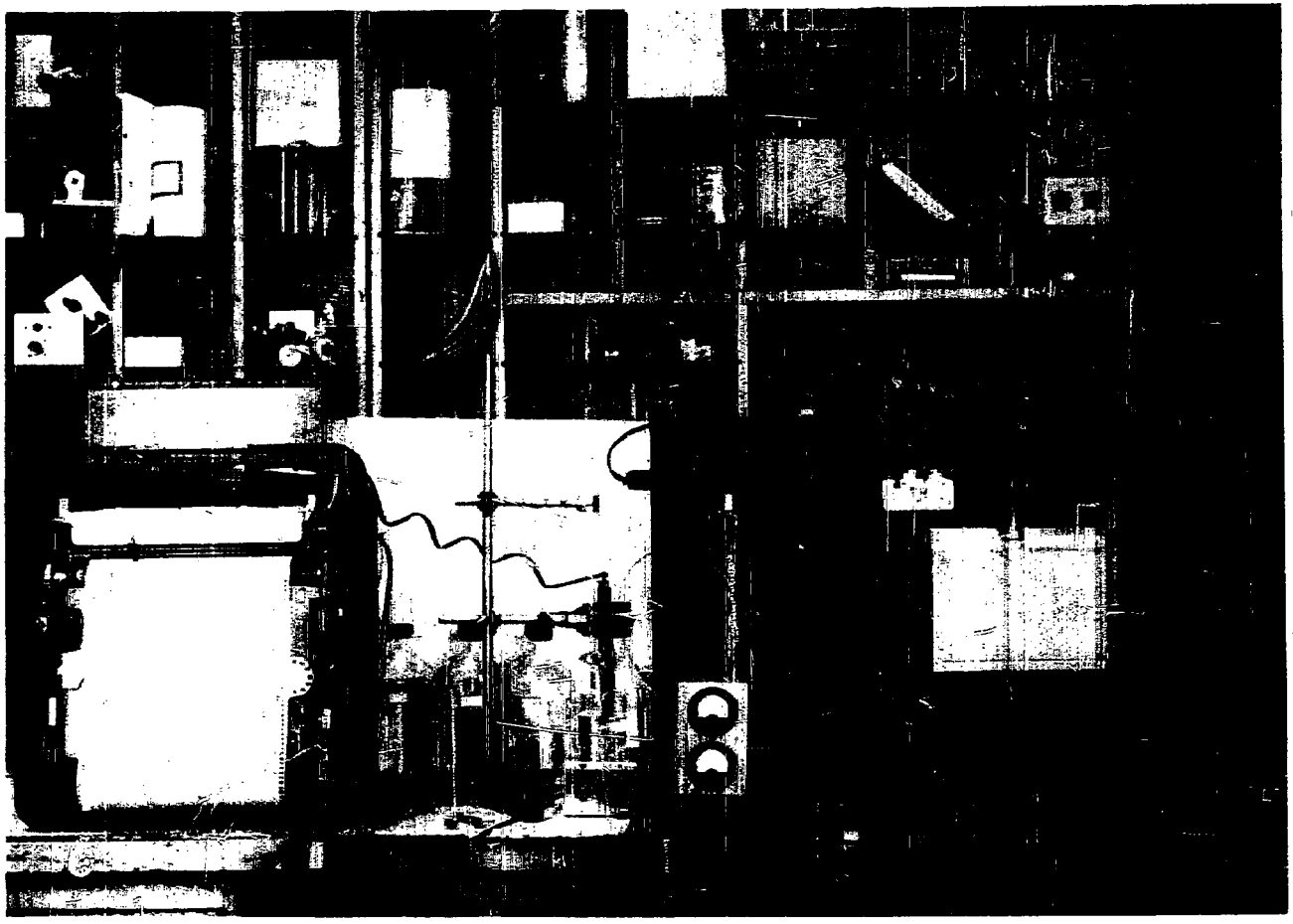

Apparatus used in calibrating the secondary standard ozone generator (lower center)

INTRODUCTION

An historical and rather complete statement of the atmospheric ozone problem has been given by Götz (1951) and Craig (1950) and hence such a statement in this writing would serve no purpose. It is well to tabulate the observations and factors, however, which, prior to this writing, were considered important to the complete ozone problem.

1. There is a seasonal variation (spring maximum and fall minimum) of the total ozone in a vertical column. Apparently there is also a late summer maximum observed at all latitudes.

2. There is a latitudinal variation of the total ozone in a vertical column with a maximum at 45° - 60° N latitude and a minimum in the equatorial regions throughout the year. A southerly latitude maximum is not clearly defined, however observations in the southern hemisphere are sparse.

3. Large day to day variations exist which are greater than the yearly variation of the monthly averages. It has been suggested that latitudinal advection, vertical motion, solar production and dissociation alone or in combination are responsible for these large day to day variations.

4. The vertical distribution of ozone has not been explained satisfactorily although the measurements and the photochemical theory show a middle stratosphere maximum.

5. The Umkehr measurements show a relationship between the vertical distribution and the total ozone in a vertical column. The Umkehr technique seems to suggest that the major variation in the total ozone occurs between 10 and 20 km. It also appears that there is a positive correlation between the potential temperature at 12, 15 and 18 km and the total ozone, while there is

a negative correlation between the tropopause height and the total ozone.

6. A correlation between total ozone and solar visibility (sun spot number) is not well established even with regard to sign.

It should be noted that in the above no mention is made of the sink at ground levels. All emphasis has been given to variations in the production rate of ozone and transport phenomena within the atmosphere. This is unfortunate since the variation in the sink strength at ground level may well dominate the variation in production at high levels. Moreover, in the above tabulation, sources of ozone other than the production from solar ultraviolet light have been omitted. It will be shown later that the production of ozone in the troposphere by electrical discharge cannot be ruled out as being insignificant.

In this writing it will be the main concern of the author to discuss the vertical distribution of ozone, the sink at ground levels which removes ozone from the atmosphere, vertical transport, ozone production via electrical discharges and measurements of the foregoing, as well as a brief explanation of the development of the chemiluminescent detector applied to the measurements. Lastly, a report on some measurements of the small ion number within the free atmosphere from ground level to balloon altitudes and the results of such measurements will be given.

The discovery of the chemiluminescent reaction between ozone and solutions of different fluorescent and non-fluorescent dyes is not new (Kearney, 1924; Biswas and Dhar, 1928). The chemiluminescent hydrazides in alkaline solution, particularly luminol, give high chemiluminescent efficiencies (Harvey, 1929; Briner, 1940; Wilhelmsen, Lumry and Eyring, 1955). Kautsky and Zocher (1921) were original in obtaining a "dry" chemiluminescent reaction between ozone and Rhodamine B adsorbed on siloxene. Bernanose and Rene (1959), used luminol for ozone determinations by adsorbing it on chromatographic paper from basic

solutions and exposing the paper to gaseous ozone. The light output was measured with a photomultiplier. It was not until 1961, however, that V. Regener brought this technique to the foreground and applied it to the measurement of atmospheric ozone. At this point Kroening and Ney (1962) began the development of a chemiluminescent ozone detector independently of the work of Regener.

THE DETECTOR

A majority of the author's work with chemiluminescent ozone detectors involved the development of the luminol silica gel detector. Luminol (5 amino-2, 3-dihydrophthalazine-1, 4-dione) dissolved in alkaline solution is adsorbed on silica gel. The resulting complex has a very high efficiency in the chemiluminescent decomposition of ozone. The efficiency of the reaction increased with increasing pH to the point where the silica gel decomposed and reverted to sodium silicate (water glass). The base used was sodium hydroxide. The reaction, however, was drastically sensitive to water vapor. Much work was done to control this reaction. Attempts to saturate, fix, or render the silica surface hydrophobic failed in the sense that the detector was never really stable enough for use in very high altitude measurements. The attractive high efficiency of the reaction, however, leads one to investigate every conceivable method that might stabilize the reaction. After this exhaustive effort failed, work was initiated on the Rhodamine B silica gel complex. Rhodamine B was chosen rather than other fluorescent or nonfluorescent dyes because the literature indicates it as being second in line of efficiency. The remainder of the detector development is restricted to Rhodamine B, not because the ideas to be presented would not apply to the use of other dyes, but rather that the author worked only with Rhodamine B. Although the precise nature of the reaction between ozone and Rhodamine B adsorbed on silica gel is not clearly understood, certain features of the reaction are evident from experiment. The reaction is heterogeneous since it takes place on the silica surface. It is not clear whether the reaction is unimolecular or bimolecular, but this really has secondary significance for its use in ozone measurements. It is clear from experiments, however, that the reaction is linear with respect to the gaseous ozone

concentration over a range of at least 1000. The mathematical formulation of a first order reaction is

$$(1) \qquad \frac{dc}{dt} = -kc$$

where c is the concentration of the reactant of interest (ozone). The order of a reaction is determined by observation. The above reaction rate is easily understood for homogeneous gas reaction. However, its application to a heterogeneous surface reaction requires a further linear relationship between the gas phase concentration and the surface concentration of the reactant. This linear relationship supposedly applies in the case of the ozone Rhodamine B-silica gel complex used in the measurements reported in this work. The activation energy required for the chemiluminescent decomposition of ozone on the above complex is not known. Suffice it to say in this respect, though, that under the temperature conditions in which the detector is used ($0^{\circ}C$ - $30^{\circ}C$), the reaction is not significantly temperature sensitive. The silica surface acts as a positive catalyst in the chemiluminescnet reaction of ozone with the fluorescent dye Rhodamine B. The silica gel provides a polar surface upon which the ozone and Rhodamine are adsorbed and on which they subsequently react. This is not unlike the manner in which alcohols and basic solutions provide surroundings for the same reaction.

Before proceeding with the chemistry of the detector, it is perhaps well that the construction and use of the detector is outlined. Rhodamine B is dissolved in either methyl or ethyl alcohol. Alcohols of higher molecular weight, except for propyl alcohol, polyhydroxyl alcohols such as glycerine and ethylene glycol, are unsuitable for chemiluminescence despite the fact that they form beautiful red-orange fluorescent solutions with Rhodamine B. This may possibly be caused by steric hindrance. In contrast to alcohols and alkaline solutions, one may also use glacial acetic acid as a solvent in which, supposedly, the

Rhodamine B becomes associated with the carboxyl group. When Rhodamine B in proper solution is contacted with ozone, light is emitted which is not greatly different from the fluorescent spectrum. Nor is the intensity of the light in the case of methyl and ethyl alcohol or acetic acid very different. However, for polyhydroxyl alcohols or alcohols of high molecular weight, the intensity is considerably diminished or undetectable. It is also interesting that the glow is considerably diminished in aqueous solution.

In preparation of a solution, .05 gm of Rhodamine B is dissolved in 50 cc of solvent. In preparation of the gel, 2 to 4 cc of solution are added to 2 gm of finely divided silica gel (200 mesh), sold commercially as acid silicic by Mallinckrodt Chemical Works. The type of silica gel used is not important as long as it is finely ground (high specific surface area) and not contaminated. The gel is then dried in a vacuum at room temperature. To complete construction of the detector, the gel is glued onto an aluminum disc (2" dia 1/16" thick). The disc is then placed 1/16" from an end window RCA 6199 photomultiplier with proper light tight fittings. The gas to be sampled is admitted to the small space between disc and photomultiplier via light tight brass tubing, coated on the inside with flat black Krylon paint. After evaporation of the Krylon propellant, a black acrylic resin remains on the tubing which does not decompose ozone appreciably. The spacing between the disc and the photomultiplier is important in order to obtain the maximum signal for a given ozone concentration and yet be consistent with the pumping apparatus. The spacing of 1/16" was found to optimum. The gas to be sampled is aspirated past the disc at a rate of approximately 500 cc per min. At very high flow rates, the signal is nearly independent of flow rate where evidently an efficiency factor comes into play. At a flow rate of 500 cc per min., practically all of the ozone is removed from the stream. Choosing a pumping speed such that all the ozone is removed prevents the possibility of the reaction rate

being controlled by diffusion to the surface. A gear pump driven by either a centrifugally governed d.c. motor or a synchronous a.c. motor provides the constant flow rate required for the measurements. The pump is placed on the downstream side of the detector.

The photomultiplier is generally operated near 1200 volts in order to provide the maximum signal as well as optimum signal to noise ratio. A 22 megohm bleeder network provides voltage to the dynodes and consists of 2.2 megohm 1/4 watt resistors between dynodes, except between the cathode and first dynode where an optimum signal to noise ratio warrants using 3.9 megohms. The photomultiplier is also magnetically and electrostatically shielded. All high voltage sections and the signal leads of the photomultiplier are potted in silastic rubber to prevent high voltage breakdown and leakage between cathode and anode.

We will now return for a moment to the chemistry of the detector. Two methods were used to verify that the reaction between Rhodamine B adsorbed on silica gel and ozone in gaseous form is linear. The first method involves the use of an ozone generator with a variable but calibrated output. The detector is subjected to the variable ozone concentration and the linearity of response is quickly checked. The second technique involves placing the detector in an atmosphere with a steady but arbitrary ozone concentration and then varying the total pressure, which can be read easily with a manometer. The partial pressure of ozone then varies in proportion to the total pressure. Such a test has been carried out in a bell jar which was connected to a vacuum pump. An initial ozone level is established and then decreased in proportion to the total pressure by the vacuum pump. In this manner, the detector has been checked for linearity over a range of partial pressures of ozone extending from about 1 μ mb up to about 1000 μ mb. Presumably the detector is linear over a much greater

range, but the need to verify this has not arisen. Linearity checks using the first technique have also been carried out and yield the same results. There is, however, one problem with the detector that has not been eliminated completely, that is, its sensitivity to water vapor. Yet, this is not surprising when one reflects upon the universal role that water plays in chemical reactions. It is, so to speak, the universal solvent without which the majority of chemical reactions would be impeded, if not prevented. The sensitivity of the silica gel-Rhodamine complex apparently changes by 25% to 100% when the partial pressure of water is changed from its vapor pressure at -72°C up to a concentration corresponding to 70% relative humidity at 25°C. The cause of the variation in sensitivity from one detector to the next for identical variations in water vapor has yet to be elucidated. Much effort without complete success has been given to this problem. A considerable improvement, on the average, has been achieved by using a substance called estersil in place of ordinary silica gel. Silica gel is very hydrophilic and is used as a drying agent. Estersil, on the other hand, is a silica gel which has been esterified (Iler, 1955). The polar end of the molecule is permanently attached to the silica surface, leaving the non-polar and extending away from the surface. The resultant surface is so hydrophobic that immersion in water does not wet the surface. Nontheless, there exists on the average a variation in the sensitivity of the detector of about 1/2 of the variation given for the ordinary silica gel. The use of a dessicant ahead of the detector to remove the water vapor immediately suggests itself. This can be done with good results if small amounts of phosphorus pentoxide (P_2O_5) are used as the dessicant. The disadvantage of other dessicants is that they decompose the incoming ozone as well as remove the water vapor. The length of time that the P_2O_5 will continue to function as a dessicant depends upon the amount of P_2O_5 present and the total water vapor influx. This can be allowed for. The other alternative is to select the detectors with

the least variation. The latter alternative has been chosen by the author. The measurements of the vertical ozone distribution will not be seriously affected because of the low water vapor content of the atmosphere, except at very low levels, and this can be allowed for if the case warrants. The water vapor problem should nontheless be investigated further in the hope that it can be eliminated eventually.

THE OZONE GENERATOR

All of the relative measurements which can be made with the chemiluminescent detector cannot be put on an absolute scale until one has an absolute standard reference source of ozone. To date, this need has not been fulfilled. A technique using long lived radioactive material is suggested from the measurements of Kroening and Nay (1962), but, at the same time, these measurements indicate that the radiation levels necessary for sufficient ozone production lie well in the lethal range. As an alternative, a secondary ozone standard has been built, using a mercury vapor lamp with a quartz envelope. This secondary standard requires periodic calibration by means of an absolute chemical method to be outlined later. The disadvantage of the secondary standard is that only its average output over a period of time, depending upon the sensitivity of the absolute chemical technique, can be determined. Short term stability is then furnished by the chemiluminescent detector to calibrate the generator at lower levels comparable to those existing in the atmosphere.

A description of the secondary standard ozone generator is now presented. The most convenient and most stable generator constructed by the author uses a General Electric 4 watt mercury vapor lamp having a 1 1/2" diameter quartz envelope. These bulbs are readily available and are used mainly for odor control. The quartz envelope bulb is epoxied to a polythylene hat such that only one half of the bulb is covered by the hat with a volume of approximately 3 cc enclosed by the hat and bulb surfaces. Into this volume, one inserts an inlet and outlet through which the air to be ozonized is passed. In general, care should be taken with all surfaces which are to come in contact with the ozone in order to reduce undesirable decomposition on any contaminated surface.

An important feature of the generator, however, is its tendency to cleanse itself. In a manner similar to which electronic tubes in critical circuits are aged for stabilization, so, in the construction of the generator, the bulb and generating chamber are aged and cleansed merely by allowing the generator to operate for a considerable length of time. Two days of continued operation generally suffice to attain stability. Yet, prior to each use of the generator, a short warm-up period is required. The output of the generator is controlled by the power supplied to the bulb. This is monitored by an ammeter and voltmeter. An autotransformer provides the variation of bulb current and voltage, and, consequently, the output of the generator. Ballast is required in series with the bulb. The output level of the above described generator generally can be varied from 5 μmb to 500 μmb if the flow rate is approximately 500 cc per min and the carrier gas is air at NTP.

CALIBRATION OF THE OZONE GENERATOR

The calibration of the generator described in the previous chapter is accomplished by the use of the absolute chemical technique described by Wadelin (1957). The ozone is passed through a solution of potassium iodide and sodium thiosulfate. The iodine is displaced as follows:

$$(2) \qquad O_3 + 2KI + H_2O \longrightarrow I_2 + O_2 + 2KOH$$

The iodine thus displaced reacts immediately with the sodium thiosulfate according to

$$(3) \qquad I_2 + 2Na_2S_2O_3 \longrightarrow Na_2S_2O_6 + 2NaI$$

The main reason for this step is to prevent the volatization and subsequent loss of the free iodine displaced by the ozone. The above solution is buffered at pH 7 or higher in order to assure the formation of no more than one mole of iodine per mole of ozone. At low pH, one would have the side reaction

$$(4) \qquad 4O_3 + 10KI + 10K^+ \longrightarrow 5I_2 + H_2O_2 + 4H_2O + 3O_2 + 10K^+$$

competing. This is eliminated by the buffer solution. In equations (2) and (3), the reaction is complete, i.e., proceeds far to the right.

Since potassium iodate (KIO_3) is sufficiently pure to be used as a standard and is stable in solution, it is now used to back titrate the amount of sodium thiosulfate remaining, the reaction being

$$(5) \qquad IO_3^- + 5I^- + 6H^+ \longrightarrow 3I_2 + 3H_2O$$

Prior to the back titration with the potassium iodate, a quantity of sulfuric acid is added so that the above reaction will proceed far to the right. A blank run (no ozone) is then made on an identical sample to provide the blank sodium thiosulfate concentration. A subtraction of the run made with the generator from the blank then yields the amount of sodium thiosulfate reacted

with the iodine which was displaced by the ozone.

The end point in the above titrations is determined amperometrically using a gold and silver amperometric probe (Gergen, 1959). The current from the probe is sent through a variable resistance. The voltage across this resistance is then measured with a 0 - 10 mv Leeds and Northrup potentiometer. The variable resistance (0 - 50K) provides a wide range of sensitivity. In this way, the end point is plotted automatically by the recorder. The ozone concentration is computed from the following equation:

$$(6) \qquad Z = \frac{(A-B) \times N \times 6 \times 22.42 \times 760 \times T \times 10^5}{2 \times F \times t \times p \times 273}$$

where A = ml of KIO_3 required for the blank

B = ml of KIO_3 required for the ozone sample

N = normality of the KIO_3

T = ambient air temperature

F = flow rate in liters/min

t = sampling time in minutes

p = ambient pressure in mm Hg

Z = ozone concentration in parts per hundred million (pphm) of air by volume. The procedure used in the above analysis is given in an appendix.

OPERATING PROCEDURE

The ozone measurements being reported in this writing are basically two-fold: 1. continuous measurements made 1 meter above the ground in Minneapolis; 2. vertical profiles obtained via balloon flights launched near Minneapolis. The ground level measurements were made over a period extending from 12/1/61 to 4/1/62. Vertical profiles of ozone concentration were made sporadically on the dates indicated in the graphs. The ground level monitor consisted of a Rhodamine B-estersil complex and photomultiplier as previously outlined and a 500 - 1600 V high voltage power supply made by the John Fluke Manufacturing Co., Seattle, Washington. A Leeds and Northrup 0 - 10 mv potentiometer with a chart paper drive of 1 1/2" per hour served as the recorder. The overall sensitivity of the system was checked on a nearly day to day basis by an ozone generator of the type previously described. Adjustments were made daily to maintain the sensitivity of the system such that a full scale chart reading corresponded to an ozone concentration of 5 parts per hundred million (5pphm) of air by volume. This was accomplished by adjusting the high voltage to the photomultiplier. Throughout this 4-months period, the sensitivity of the detector decreased by about a factor of 5 because of the oxidation of the Rhodamine and contamination of the detector by air pollutants.

The detectors used in the high altitude soundings were of the same type as that used in the ground monitor. The type of high voltage power supply used in the soundings is indicated schematically in figure 1. These supplies satisfied strict stability specifications. The gear pump is driven by a centrifugally governed d.c. motor, providing a constant volumetric flow rate independent of the pressure. The complete flight detector weighs only 1 1/2 lbs. The detector output is designed to work directly into the standard 1680 mc Weather Bureau radiosonde system.

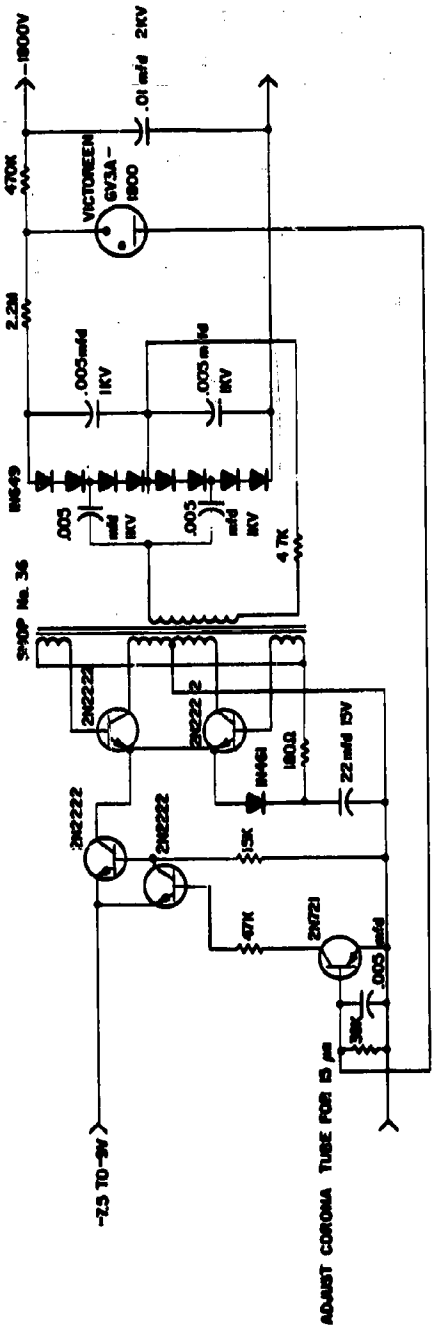

Fig. 1. Schematic diagram of the type of high voltage power supply used with the balloon borne ozone detector.

PHOTOCHEMISTRY OF ATMOSPHERIC OZONE

Since the seasonal variation in the total atmospheric ozone in a vertical column is 180° out of phase with the sun, little hope remains for the photochemical theory alone in explaining this observation. Transport phenomena and other sources of ozone are undoubtedly necessary in the complete explanation. Before considering other processes, it is convenient to consider the photochemical theory. The photochemical theory originated with Chapman (1930), was followed up by Wulf and Deming (1936), and, finally, Craig (1950) has given much consideration to the problem. A brief sketch of the theory is presented below.

The dissociation of the oxygen molecule is taken as the primary step in the eventual formation of atmospheric ozone. This proceeds according to the following scheme discussed originally by Chapman.

a) $O_2 + h\nu \longrightarrow O + O$ $\quad \lambda < 2400$ A°

b) $O + O + X \longrightarrow O_2 + X$

c) $O + O_2 + X \longrightarrow O_3 + X$

d) $O + O_3 \longrightarrow 2O_2$

e) $O_3 + h\nu \longrightarrow O_2 + O$ $\quad \lambda < 11{,}000$ A°

The importance of three body collisions relative to the two body collisions decreases as one goes to lower pressures. That is, the processes

f) $O + O \longrightarrow O_2 + h\nu$

g) $O + O_2 \longrightarrow O_3 + h\nu$

will dominate b) and c) high in the atmosphere.

Let n_1, n_2, n_3, and n be the O_1, O_2, O_3 and air concentrations respectively. Denote the recombination coefficient for processes b), c) and d) by k_{11}, k_{12}, and k_{13} respectively. Then we may write the rate equations for

n_1, and n_3 as follows:

$$(7) \qquad \frac{dn_1}{dt} = 2J_2n_2 + J_3n_3 - 2k_{11}n_1^2n - k_{12}n_1n_2n - k_{13}n_1n_3$$

$$(8) \qquad \frac{dn_3}{dt} = \quad - J_3n_3 \quad + k_{12}n_1n_2n - k_{13}n_1n_3$$

where J_2 and J_3 represent quantities proportional to the solar radiation available for processes a) and e) respectively.

In the main part of the ozone layer process d) is much smaller than process c). This is visualized by the ratio of the appropriate terms as follows:

$$(9) \qquad \frac{k_{12}n_1n_2n}{k_{13}n_1n_3} \approx \frac{12n_2}{n_3}$$

Eucken and Patat (1936) have measured the ratio k_{12}/k_{13} which is reproduced in figure 2. Choosing $T = -80^{\circ}C$ and $n = 3 \times 10^{18}$ equation (9) is verified. Furthermore, Chapman (1955) has given the values of K_{12} and k_{11} as

$$(10) \qquad \begin{aligned} k_{12} &\simeq 5 \times 10^{-36}\, T^{1/2} \text{ cm}^6/\text{sec} \\ k_{11} &\simeq 5 \times 10^{-34}\, T^{1/2} \text{ cm}^6/\text{sec} \end{aligned}$$

It should be kept in mind that they are only approximate values as yet to be verified by experiment. Using these values one likewise finds that term b) is negligible in the main ozone layer. Setting $2J_2n_2 = 2Q_2$ and $J_3n_3 = Q_3$ we get from equation (7) at equilibrium that

$$(11) \qquad n_1 = \frac{2Q_2 + Q_3}{k_{12}n_2n}$$

In addition for the case $\frac{dn_1}{dt} + \frac{dn_3}{dt} = 0$ we get

$$(12) \qquad n_3 = \frac{Q_2}{k_{13}n_1} = \frac{k_{12}n_2n}{k_{13}(2 + Q_3/Q_2)} \quad \text{or} \quad (13) \quad n_3 = \frac{k_{12}\, n_2\, n}{k_{13}(1 + Q_3/Q_2)}$$

depending upon whether or not term d) is neglected. Under the conditions of interest $Q_3 >> Q_2$. The ratio Q_3/Q_2 is a complicated function of altitude and Q_3

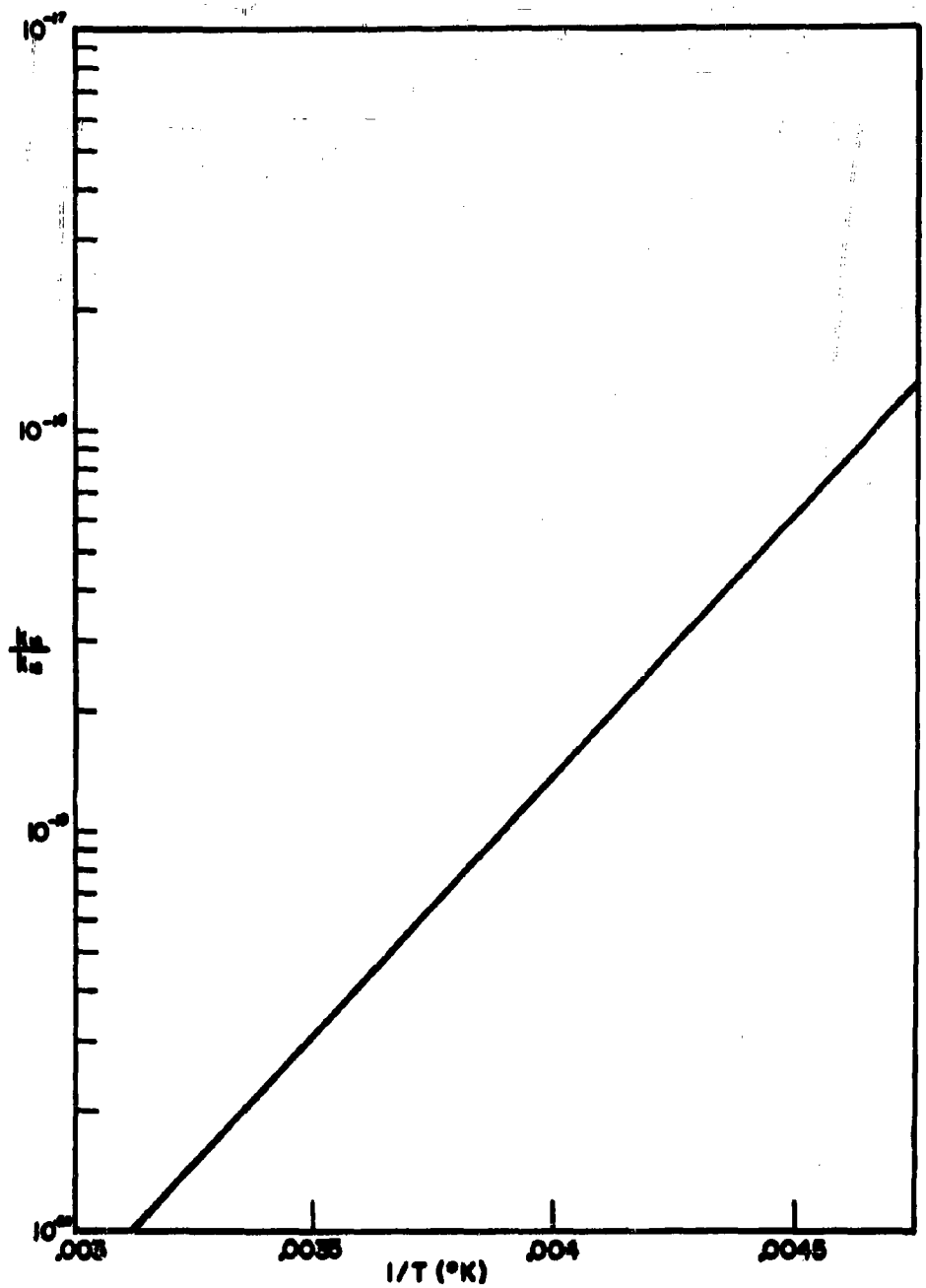

Fig. 2. The ratio of rate coefficients k_{12}/k_{13} vs 1/T(°K).

depends on n_3. Hence, a direct calculation is impossible. Wulf and Deming get the vertical distribution using successive approximation. Since the product $n_2 n$ has a scale height of one half of that for the atmosphere, one would expect n_3 to decrease rapidly above the maximum. The decrease of n_3 above the maximum, however, depends also on the ratio Q_3/Q_2 and hence on zenith angle. Craig (1950) gets a scale height of approximately one half of the atmospheric scale height for the sun in the zenith and approximately the atmospheric scale height for a zenith angle of 67°. Equation (13) can be reduced to the form

$$n_3^2 J_3 + n_3 n_2 J_2 - 3k n_2^3 J_2 = 0 \tag{14}$$

where

$$k = \frac{k_{12}}{k_{13}} \tag{15}$$

with

$$n \approx n_2 + 1/2\, n_{N_2} = 3n_2 \tag{16}$$

n_{N_2} = nitrogen concentration

Solving equation (14) for n_3 and using the approximation that $J_2 \ll 12\, J_3 J_2 n_2 k$, there results

$$n_3 = n_2 \sqrt{\frac{3k J_2 n_2}{J_3}} \tag{17}$$

The equilibrium time can be estimated from

$$\frac{d(n_1 + n_3)}{dt} = 2 n_{n_2} J_2 - 2k_{13} n_3 n_1 \tag{18}$$

Since $n_3 \gg n_1$ and the last term on the right of equation (18) is small, we get as a first approximation that

$$n_3(t) = n_3(0) + 2 n_{n_2} J_2 t \tag{19}$$

From this, the time of half restoration is estimated as

$$t_{\frac{1}{2}} \simeq \sqrt{\frac{kn}{J_2 J_3}} \tag{20}$$

This is a drastic simplification, however, since the time of half restoration depends markedly on the initial value of n_3. This has been treated thoroughly by Craig (1950), and Table I tabulates the time constants estimated by him.

The times given (Δt) apply to changes from 100 n_{3e} to 2.57 n_{3e}, 2.57 n_{3e} to 1.50 n_{3e}, 1.50 n_{3e} to 1.20 n_{3e}, 1.20 n_{3e} to 1.08 n_{3e} or the reciprocals of the foregoing as the case may be. n_{3e} is the photochemical equilibrium value. Cases I and $\bar{V}$ are for zenith angles of 0° and 67° respectively and no dependence of the oxygen absorption coefficient on pressure. Case II is for zenith angle of 0° but with a pressure dependence of $p^{1.55}$ for the oxygen absorption coefficient.

TABLE I

	Δt (days)		
Height (km)	Case I	Case II	Case $\bar{V}$
38	.15	.22	.34
35	.60	.93	2.1
32.5	2.9	3	8.9
30	13	11	52
27.5	51	30	278
25	175	80	1,570
22.5	650	184	4,290
20	3,000	515	240,000
17.5	19,900	1,470	
15	84,000	5,100	

The case for better agreement between the total ozone measurements and the predictions of photochemical equilibrium theory rest squarly on the following:

1. The dependence of the oxygen absorption coefficients in the range

1950 A° to 2150 A° upon pressure. The work of Heilpern (1941, 1946) gives a pressure exponent of 1.55 at 2144 A° over the range of pressure 683 mm Hg to 148 mm Hg. The pressure dependence of the absorption coefficient in the range 1950 A° - 2150 A° dominates the production of ozone in the range 20 km to 30 km. It is precisely in this range of altitude that the majority of change with zenith angle of the sun occurs in the total ozone in photochemical equilibrium.

2. An inclusion in the photochemical theory of more representative temperature profiles than heretofore have been used. Again the region of importance is 20 - 30 km and above. The necessity for this lies in the extreme temperature dependence of the ratio of rate coefficients k.

Some reasons for the above statements will now be given. With regard to the first, it is convenient to consider the work of Craig (1950). Craig has computed the total ozone expected at 45° N latitude for various solar zenith angles. The total amounts are: ($Z = 22°$), .262 cm; ($Z = 45°$), .196 cm; and ($Z = 67°$), .185 cm or .085 cm, depending, respectively, upon whether the oxygen absorption coefficient is or is not pressure dependent. Hence, the total ozone obtained is either moderately or drastically different depending on whether the absorption coefficient is or is not pressure dependent.

In a determination of the effect of k on the total ozone, Craig used only a small seasonal difference of temperature in the stratosphere. For example, a temperature difference of only about 4°C was taken as representative for the difference of air temperature between the winter and summer stratosphere at 45° N latitude. Furthermore, an isothermal stratosphere was assumed for both winter and summer. This would lead to a variance in k of only about 20%. However, in actual fact, the temperature difference between summer and winter at 45° N at 10 mb is approximately 20°C. This would produce a variation in k amounting to about 320%. The two effects tend to cancel each other. That is, greater zenith angles leading to smaller total ozone values are accompanied by

larger values of k leading to larger ozone concentrations. Furthermore, it should be pointed out that the observed ozone maximum, at least at 45° N, is much lower than that predicted by Craig. This lends more weight to the seasonal variation of k effecting the total ozone value.

3. Measurements of the solar flux below 2200 A°. All of the calculations given by Craig are based on an extrapolated flux in this most important part of the solar spectrum as far as ozone production is concerned.

In spite of the above, it appears that the photochemical theory alone will not suffice to explain the observations.

In contrast to the photochemical production of ozone just outlined, Briner (1959) has tentatively suggested the following mechanism for the production of O_3 by mercury vapor lamps by radiation in the region 2000 A°→2100 A°.

$$(O_2)_2 + h\nu \longrightarrow O_3 + O$$

followed by rapid attachment of the odd oxygen atom

$$O + O_2 + M \longrightarrow O_3 + M$$

yielding an overall quantum efficiency of 2 ozone atoms per photon absorbed. The quantity of O_4 available in the atmosphere is uncertain; however, it has been reported in the telluric absorption spectrum (Goldberg, 1953). The argument against its existence in any quantity is that its binding energy is comparable to thermal energies. The proportion of O_4 should be very pressure and temperature dependent. For example, it constitutes approximately 50% of liquid oxygen. It is also interesting along these lines that the absorption coefficient for oxygen in the critical range near 2100 A° is pressure dependent with a varying exponent. For example, for the range 148 - 663 mm Hg at 18°C the exponent is 1.55, while from 50 - 130 atmospheres it is 2.12.

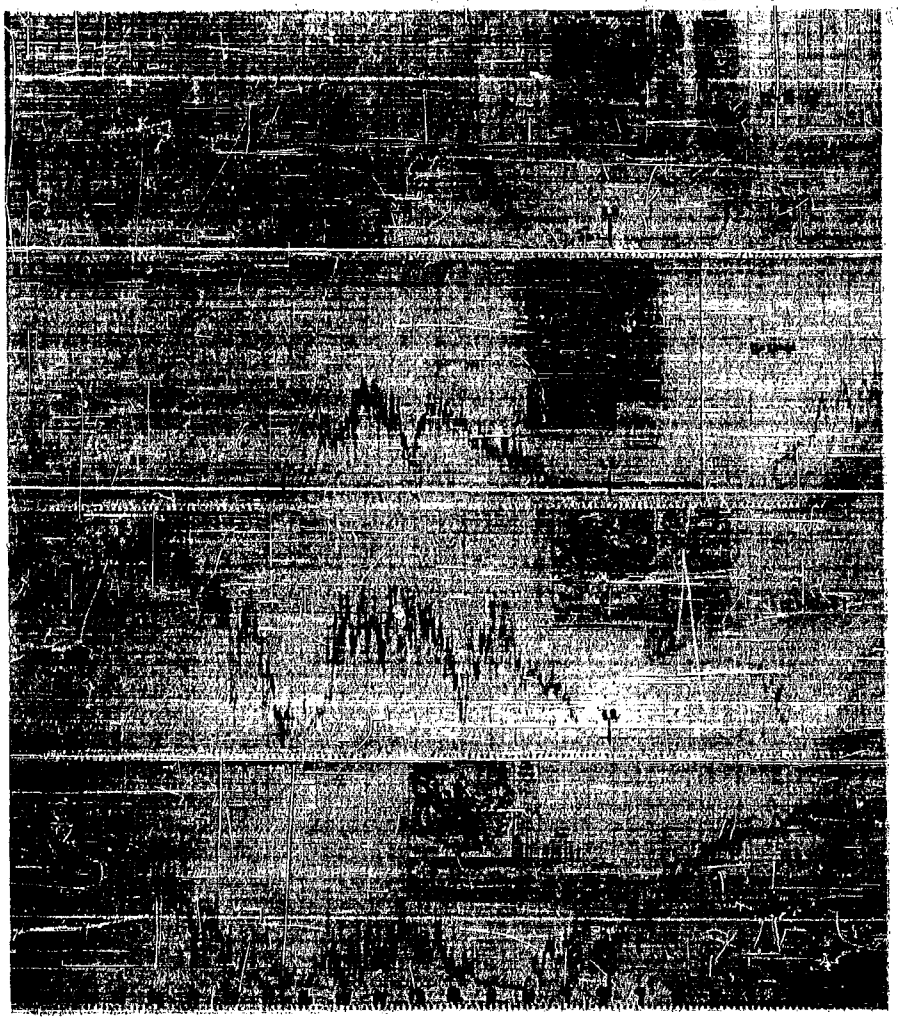

Fig. 3. Ozone measurements 1 m above the ground at Minneapolis on Dec. 19, 20, 21 and 22, 1961.

RESULTS

The data presented and discussed in this chapter were accumulated solely with the chemiluminescent detector. They will be divided into two parts: 1. ground level measurements; 2. vertical ozone profiles obtained on balloon flights. Since the volume of ground level data is so large, only a small portion of it is presented.

1. Ground level measurements. The surface measurements were made in Minneapolis at a height of 1 meter above the ground and extended from December 1, 1961 to March 1962. The most pronounced effect observed is the occurence of a diurnal variation on almost all days but to a varying degree. This is shown in figures 3 and 4. The extent of the diurnal variation is determined in the main by the magnitude of the surface level winds and the sky cover. This is understandable in terms of the two types of mixing processes which are responsible for the arrival of ozone at the surface: mechanical mixing, and thermal instability arising frim surface heating by the sun. Clear nights with low wind are accompanied by low ozone concentration near the surface. Clear days with low wind, on the other hand, are not necessarily accompanied by low ozone concentration because of thermal mixing. Cloudy days and nights are associated with a small diurnal variation and an overall lower concentration of ozone. The overall dependence of the ozone level 1 meter above the ground on the surface winds for Minneapolis throughout the month of December is given by the scatter diagram in figure 5. Since the surface wind measurements were those recorded by the U.S. Weather Bureau at Wold-Chamberlain airport while the ozone measurements were made at the University of Minnesota, a great deal of scatter is to be expected. However, an average relationship

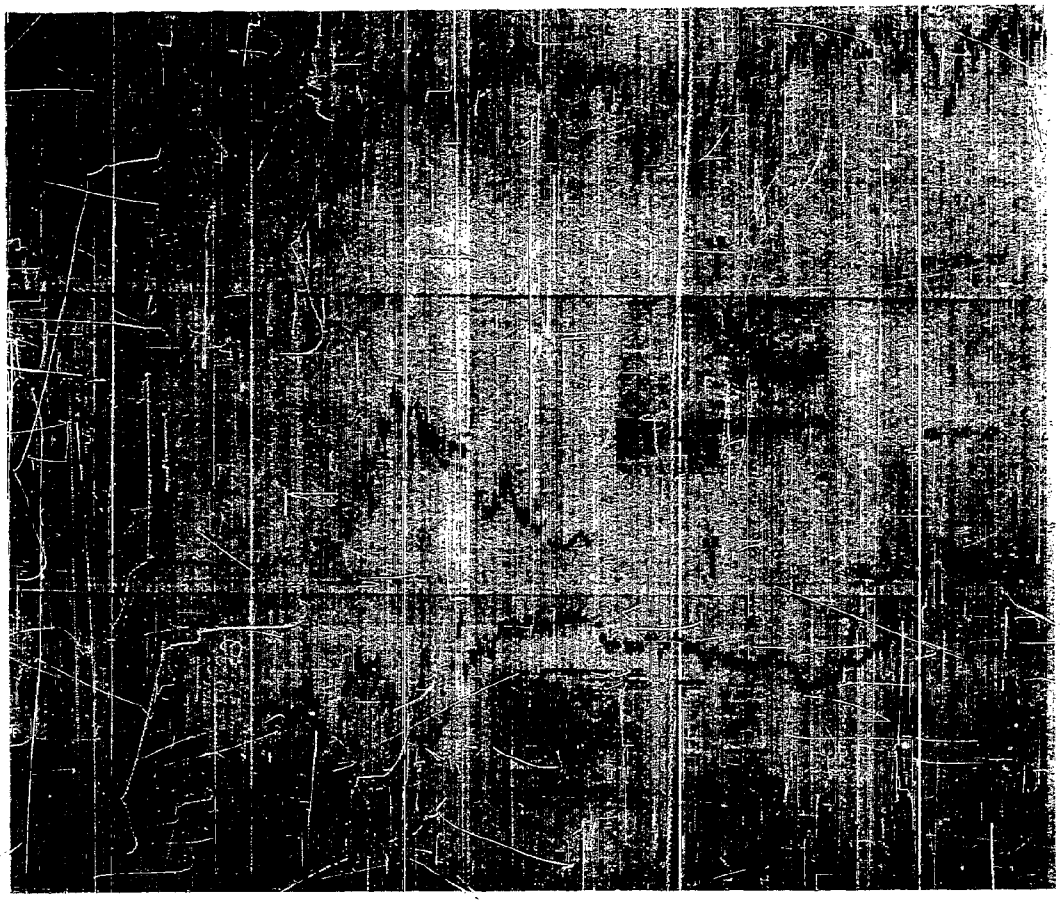

Fig. 4. Ozone measurements 1 m above the ground at Minneapolis on Dec. 23, 24 and 25, 1961.

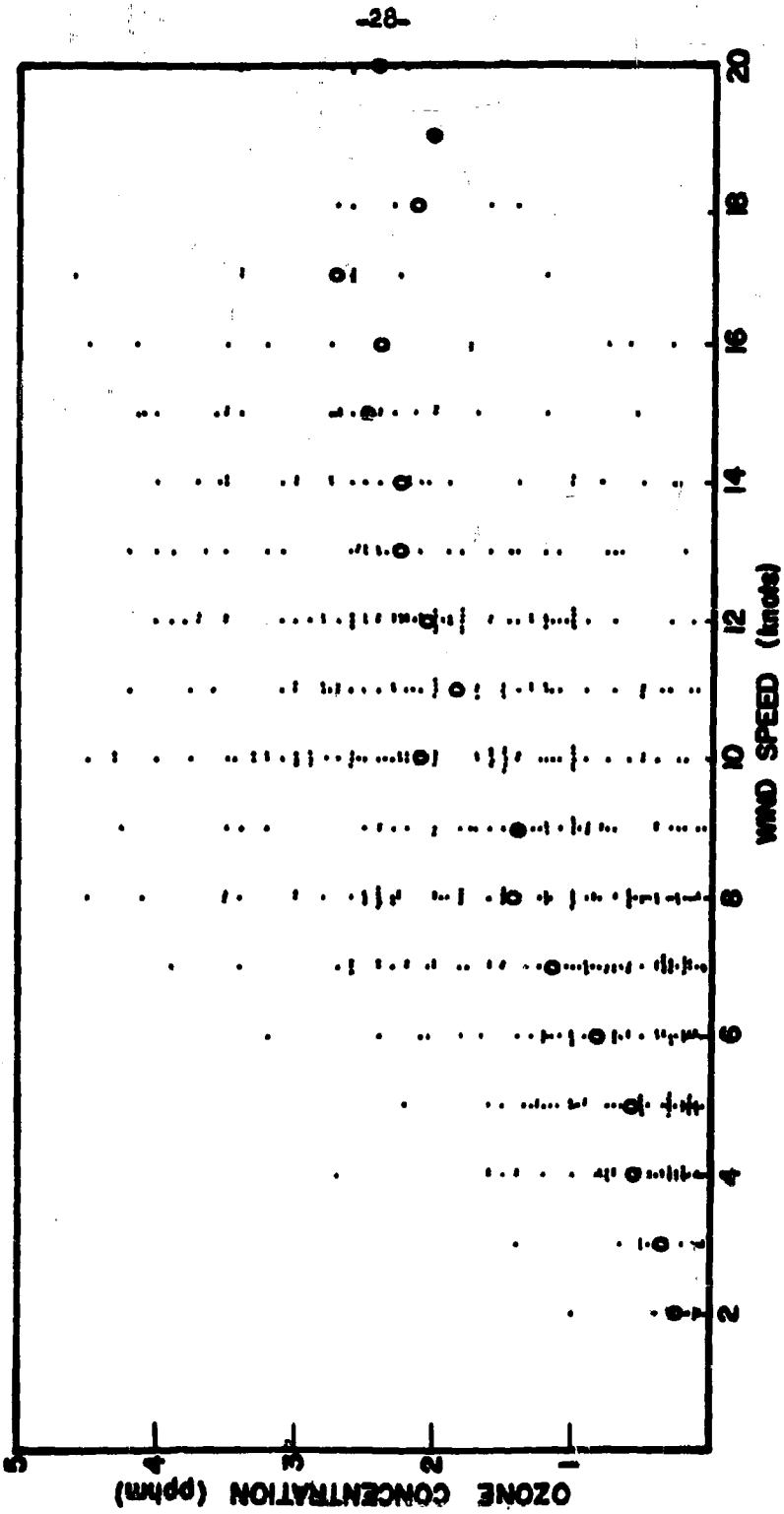

Fig. 5. Scatter diagram of surface wind speed vs the ozone concentration 1 m above the ground at Minneapolis.

between surface wind and ozone concentration is clear. None of the ideas in this section make sense without the existence of an ozone sink at the earth's surface, which is continually removing ozone from the atmosphere. The large diurnal variation observed near the surface prompted measurements of the vertical distribution by means of a tethered balloon which could be raised and lowered through the lower layer. This work was done and reported by Kroening and Ney (1962). For convenience, it is reproduced in figure 6. The graph shows three vertical distributions of ozone spaced in time shortly after sunset which were obtained at the Anoka County airport on June 20, 1961. It was a clear night with low surface winds. The vertical temperature distribution was monitored at the same time. The model adopted from this data is that when conditions allow a temperature inversion to form near the surface, the process of decomposition removes the ozone from the layer near to the surface. This provides a simple and direct measurement of the sink strength. From the data in figure 6, Kroening and Ney (1962) have deduced a sink strength of 6×10^{10} atoms/cm^2 sec by merely noting the quantity of ozone removed and the time required for this to occur. Although this value of the sink strength is really an average value over a specified time interval, it is difficult to allow a variance of more than a factor of 2 in the above estimate.

After establishing the value of the sink strength as in the above, it is possible to determine the kinetic-theory properties associated with this sink. Since the eddy diffusivity in the atmosphere near the ground is much larger than the kinetic theory value, the vertical ozone distribution is determined completely by eddy diffusion. Yet, in the last few mean free paths kinetic-theory phenomena must take over. Thus, the value of the sink strength can be used to determine the number of collisions required before decomposition occurs. The appropriate equation is:

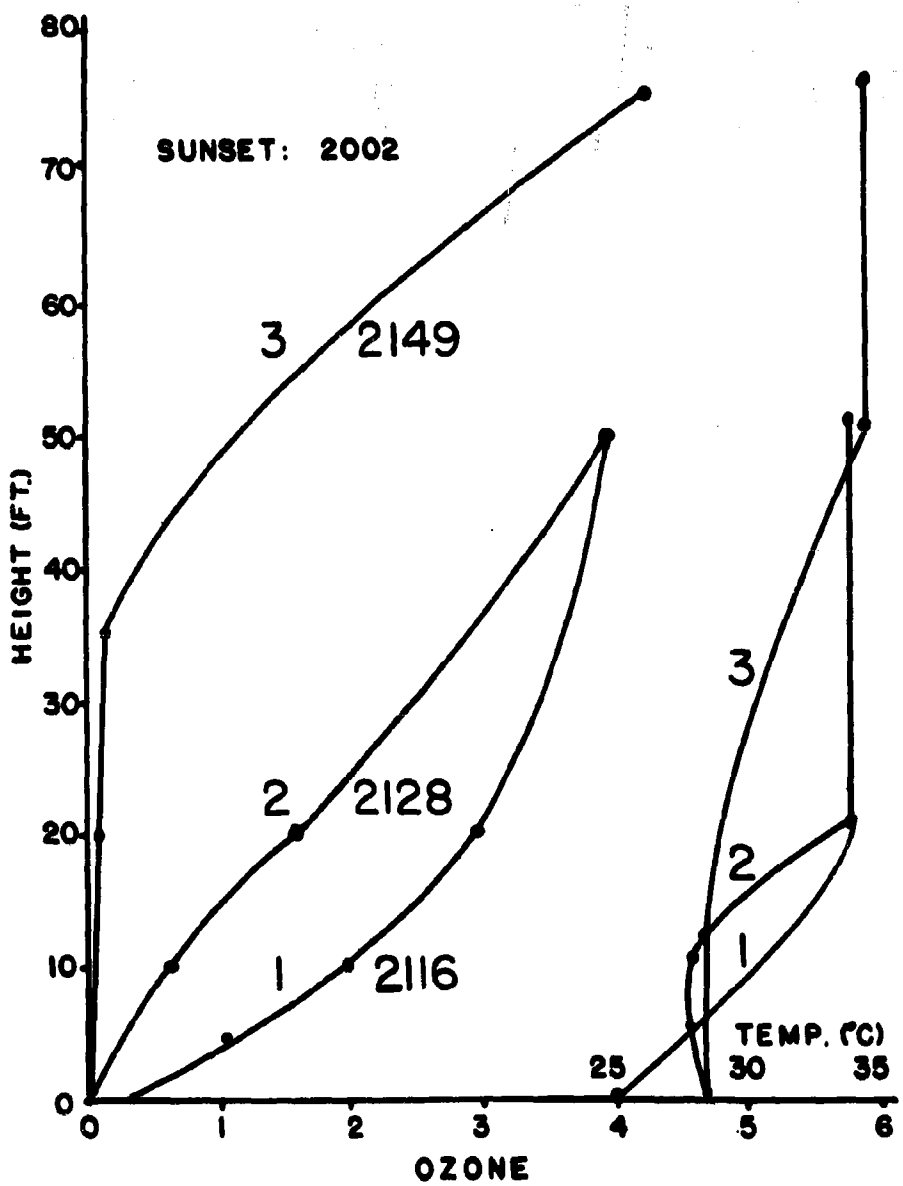

Fig. 6. The ozone concentration and air temperature vs altitude in the lower surface layers shortly after sunset on June 20, 1961.

$$(21) \qquad 1/4 n_3 \bar{v} f = 6 \times 10^{10} \frac{\text{atoms}}{\text{cm}^2 \text{sec}}$$

where n_3 is the number density of ozone molecules, $\bar{v}$ is the mean molecular velocity and f is the fraction of collisions with the surface leading to decomposition of an ozone molecule. Putting in the appropriate numbers

$$n_3 = 6 \times 10^{11}/\text{cm}^3$$
$$\bar{v} = 3.6 \times 10^4 \text{ cm/sec}$$

f is determined to be approximately 10^{-5}. Hence, only one collision in 100,000 is effective in decomposing an ozone atom and removing it from the atmosphere. This is characteristic of many chemical reactions in which activation energies can be overcome only by molecules on the tail of the maxwellian destribution in order for the reaction to proceed. The value of $f = 10^{-5}$ falls within the range of values measured for ordinary laboratory materials. For example, f for black rubber is 2×10^{-4}, while for mayon tubing $f = 2 \times 10^{-8}$. Mayon tubing is so resistant to the decomposition of ozone that it can be used in ozone plumbing with negligible loss.

With the value of f at hand, it is now possible to back track and make the following point. In the above discussion, it was clearly demonstrated that the decomposition rate of ozone near the earth's surface is diffusion controlled. The mathematical formulation of this is as follows:

$$(22) \qquad \Gamma = D \frac{dn_3}{dz}$$

where Γ is the vertical diffusive flux of ozone, D is the vertical eddy diffusion coefficient and $\frac{dn_3}{dz}$ is the vertical gradient of the ozone concentration. If the above vertical flux is equated to the strength of the sink, we obtain

$$(23) \qquad D \frac{dn_3(z)}{dz} = 1/4 \, n_3(0) \bar{v} f$$

This equation relates the vertical eddy diffusivity, the vertical ozone con-

centration gradient in a simple manner once f is known. It can be applied where vertical diffusion is the sole transfer process and only in that part of the atmosphere where ozone is a conservative constituent. Under steady conditions, we would then have the production at high levels balanced by the destruction at the surface. In this state, a quantity of ozone would be stored in the atmosphere which depended solely on the production at high levels, the eddy diffusivity and the product $\bar{\nu}f$.

Equation (23), although written for the steady state, lends some insight into the non-steady state process near the surface. If conditions at some locality are such that $\bar{\nu}f$ does not change appreciably over a certain time interval but the sink strength changes in accordance with $n_3(0)$, it is possible to generate high ozone concentrations in the troposphere near the ground. If there is a change of the steady state conditions to which (23) applies to the case where the sink effectively vanishes, as would be in the abrupt formation of an inversion near the ground or stagnant air masses, the ozone concentration immediately begins to increase above the inversion or stagnant air mass. If these conditions persisted long enough, the ozone would back up, so to speak, all the way through the atmosphere. However, the majority of these situations are short termed, and, furthermore, horizontal transport will wash out the effect by horizontal diffusion and advection. Yet, there should be an average effect of this kind for the whole atmosphere, and, certainly, it should be visible in the individual cases as the following calculation shows:

$$\Delta n_3(z_o) = \frac{\Gamma \Delta t}{\Delta z} \qquad (24)$$

Substituting the appropriate number, equation (24) yields

$$\Delta n_3(z_o) = \frac{6 \times 10^{10} \frac{\text{atoms}}{\text{cm}^2\text{sec}} \times 10^5 \text{sec}}{10^5 \text{cm}} = 6 \times 10^{10} \frac{\text{atoms}}{\text{cm}^3}$$

This calculation is consistent with the downward flux and the vertical eddy

diffusivity in the troposphere. The build up is considered to take place in the time interval of a day and within a layer 1 km thick. It was also assumed that the ozone mixing ratio increases by 10% per km. The data shown in figures 3 and 4 are consistent with such an explanation. The graphs include days (12/20/62 and 12/24/62) when the resultant wind at the surface is very small. This is preceded and followed by days in which there was good movement. The days after the day of low resultant wind are accompanied by higher than normal ozone at ground level. This trend is the same for 9 out of 13 instances on record. Hence, it is clearly brought out once again that the ozone content of the atmosphere is dependent on surface conditions via a diffusion controlled process in the layers near to the earth's surface. Still there is another point to be made regarding the sink strength, and it is probably the most important. One is forced to consider the variation of $\bar{v}f$ in the sink strength. Although $\bar{v}$ is proportional to $T^{1/2}$ where T is the ambient surface temperature in degrees Kelvin, the factor f will have an exponential temperature dependence and will certainly depend on the nature of the surface. But it is not obvious how one can handle this last variance. For the discussion, it will be assumed that there is some substance, perhaps water, which may be considered as representative for the whole surface. That this assumption is valid might be indicated by a northern-southern hemisphere total ozone difference since the northern hemisphere contains much more land mass. It will also be assumed that the sink strength determined at Minneapolis from figure 6 is representative of the activation energy for decomposition at that temperature and that this activation energy is the same for the whole northern hemisphere. Thus,

$$(25) \qquad e^{-E_o/kT} = 10^{-5}$$

if there is no steric hindrance in the decomposition process. E_o is the energy of activation, T is the absolute temperature and k is the Boltzmann factor. With $T = 300^{\circ}K$ the solution of (25) is $E_o = .3$ ev. With E_o in hand, we can con-

struct the temperature dependence of f. This is given in figure 7. Hence, we finally have a means of treating the variability of the sink strength. Assuming an activation energy of .3 ev, equation (25) predicts a variation of a factor of 300 for a temperature change of 200°K to 300°K. Clearly, then, the sink strength must be included in any equilibrium theory of atmospheric ozone. We will now proceed to estimate the effect of the sink on the total ozone. Rewriting equation (23) so as to allow for variation in air density results in

$$(26) \qquad nD \frac{d\nu}{dz} = 1/4\, n_3(o,\lambda)\bar{v}f$$

where $$\nu = \frac{n_3}{n}$$

If 1) source and sink are in equilibrium

2) horizontal transfer is unimportant

3) furthermore molecular diffusion is unimportant

4) we consider only that part of the atmosphere in which ozone is a conservative constituent, then integration of (26) yields

$$(27) \qquad n_3(z,\lambda) = n_3(0,\lambda)e^{-z/H} + e^{-z/H} \int_o^z \frac{n_3(o,\lambda)\bar{v}f}{4D\, e^{-s/H}}\, ds$$

for the vertical ozone distribution. Integrating (27) between z = o and z = h gives the total ozone in a 1 cm^2 column of height h as

$$(28) \qquad N_3(h,\lambda) = n_3(o,\lambda)H(1-e^{-h/H}) + \int_o^h e^{-z/H} \left[\int_o^z \frac{n_3(o,\lambda)\bar{v}f}{4De^{-s/H}}\, ds \right] dz$$

In the above $n = n_o e^{-z/H}$ hydrostatic equation

λ = latitude

H = atmospheric scale height

D = vertical eddy diffusivity

$n_3(z,\lambda)$ = ozone number density

$N_3(h,\lambda)$ = total ozone between z = o and z = h

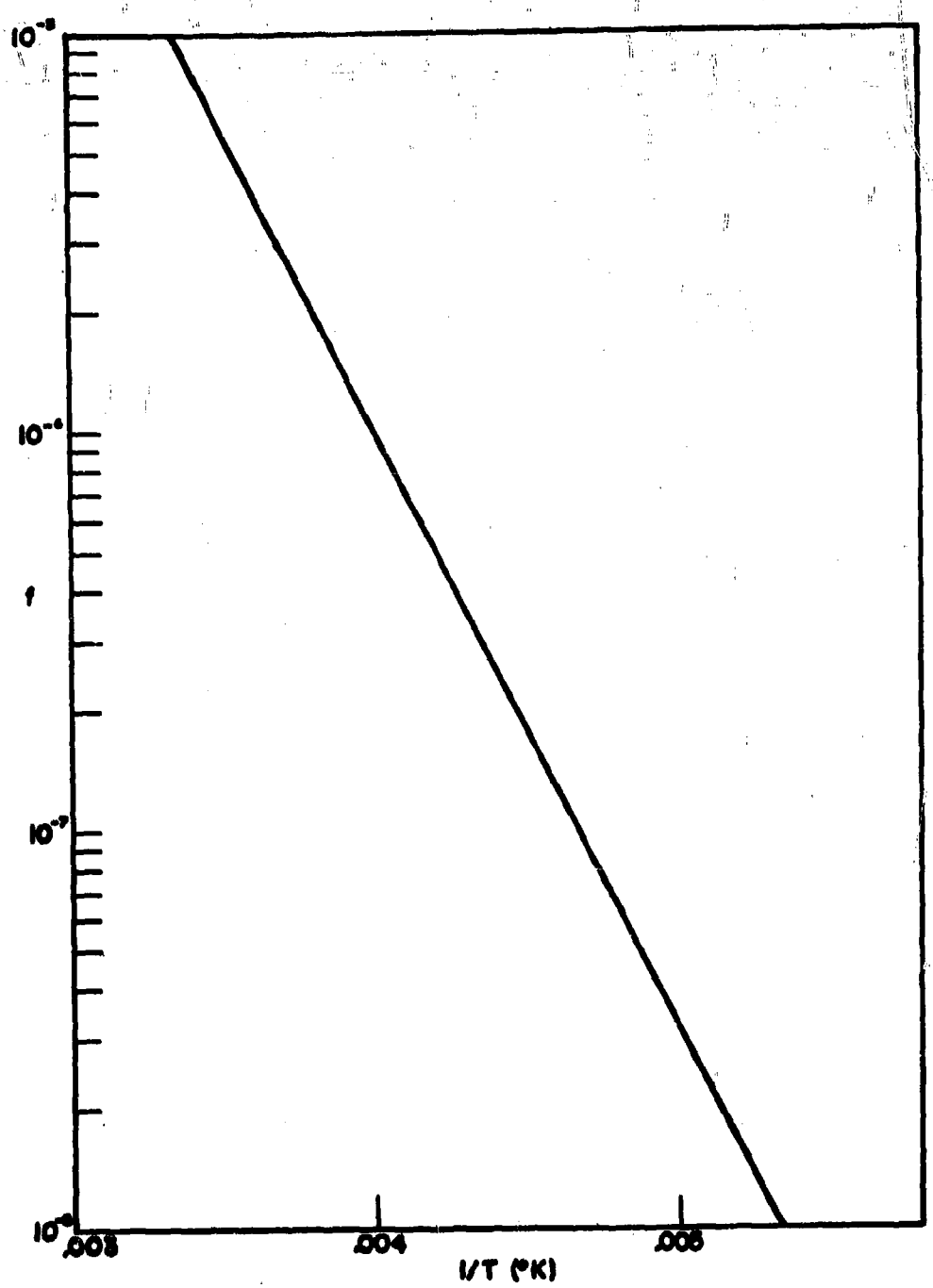

Fig. 7. The ozone sink parameter f vs 1/T.

Taking h = 4H

$$(29) \qquad N_3(4H,\lambda) \simeq n_3(o,\lambda)H + \int_o^{4H} e^{-z/H}\left[\int_o^z \frac{n_3(o,\lambda)\bar{v}f}{4De^{-s/H}}\,ds\right]dz$$

If it is now assumed that the source strength and D are independent of latitude, then the last term on the right of (29) is a constant. The first term then represents the ozone stored in the atmosphere to compensate for the variation in f. This term will be dependent on latitude.

$$(30) \quad \Delta N = N_3(4H,\lambda) - N_3(4H,0) = H\left[n_3(o,\lambda)-n_3(o,0)\right] = Hn_3(o,0)\left[\frac{n_3(o,\lambda)}{n_3(o,o)} - 1\right]$$

The latitudinal dependence of this term is shown in figure 8, curve B, computed from London's (1957) mean temperatures and under the assumption that the product $n_3(o,\lambda)$ f is a constant. If curve B is weighted according to the yearly mean insolation as given by Fritz (1951), curve C is the result. In a similar manner one can obtain the seasonal variation

$$(31) \qquad \Delta N_s = N_3(4H,\lambda)_{winter} - N_3(4H,\lambda)_{summer}$$

The ratio $\Delta N_s/\Delta N$ of the seasonal variation to the mean latitudinal variation is given in figure 8, curve A. Suffice it to say, however, that the magnitude of these terms is small compared to the total ozone observed. This is shown in figure 9 which gives the observed yearly mean latitudinal variation while the solid curve gives the expected variation from the above analysis, assuming the total ozone at the equator is 240 milli-atmo-cm and that $n_3(o,o) = 4\times10^{11}/cm^3$. The seasonal variation, while small, is in phase with the temperature. Although the above considerations appear unimportant regarding total ozone, they still predict a latitudinal variation in the ozone concentration in the troposphere of a factor of about six from the equator to the pole.

Hence, we must look for variations occuring in the second term on the right side of equation (29). This term can be written under the previous assumption

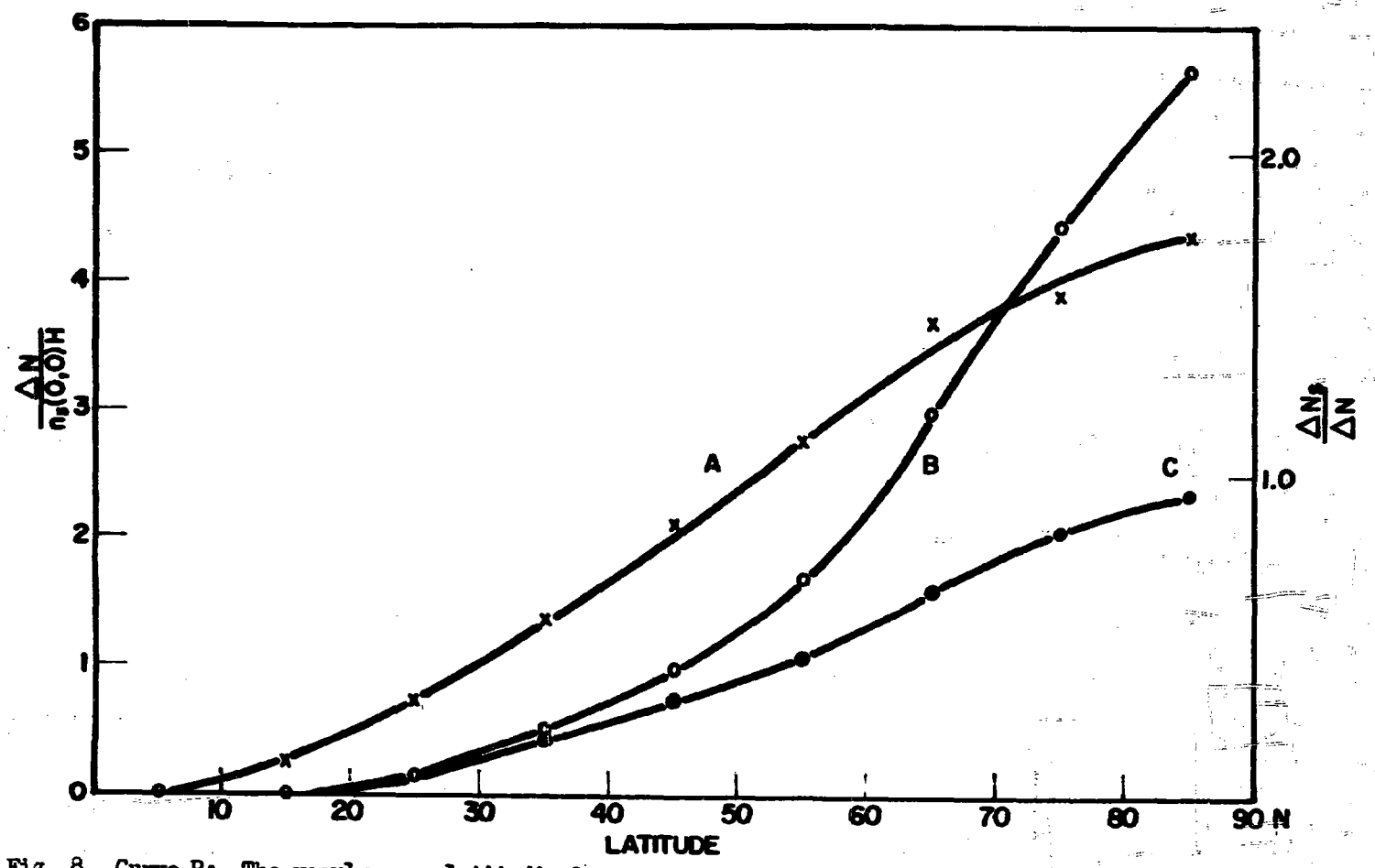

Fig. 8. Curve B: The yearly mean latitudinal variation of total ozone for constant source. Curve C: curve B weighted according to the mean insolation. Curve A: The seasonal variation of total ozone relative to the yearly mean latitudinal variation of total ozone.

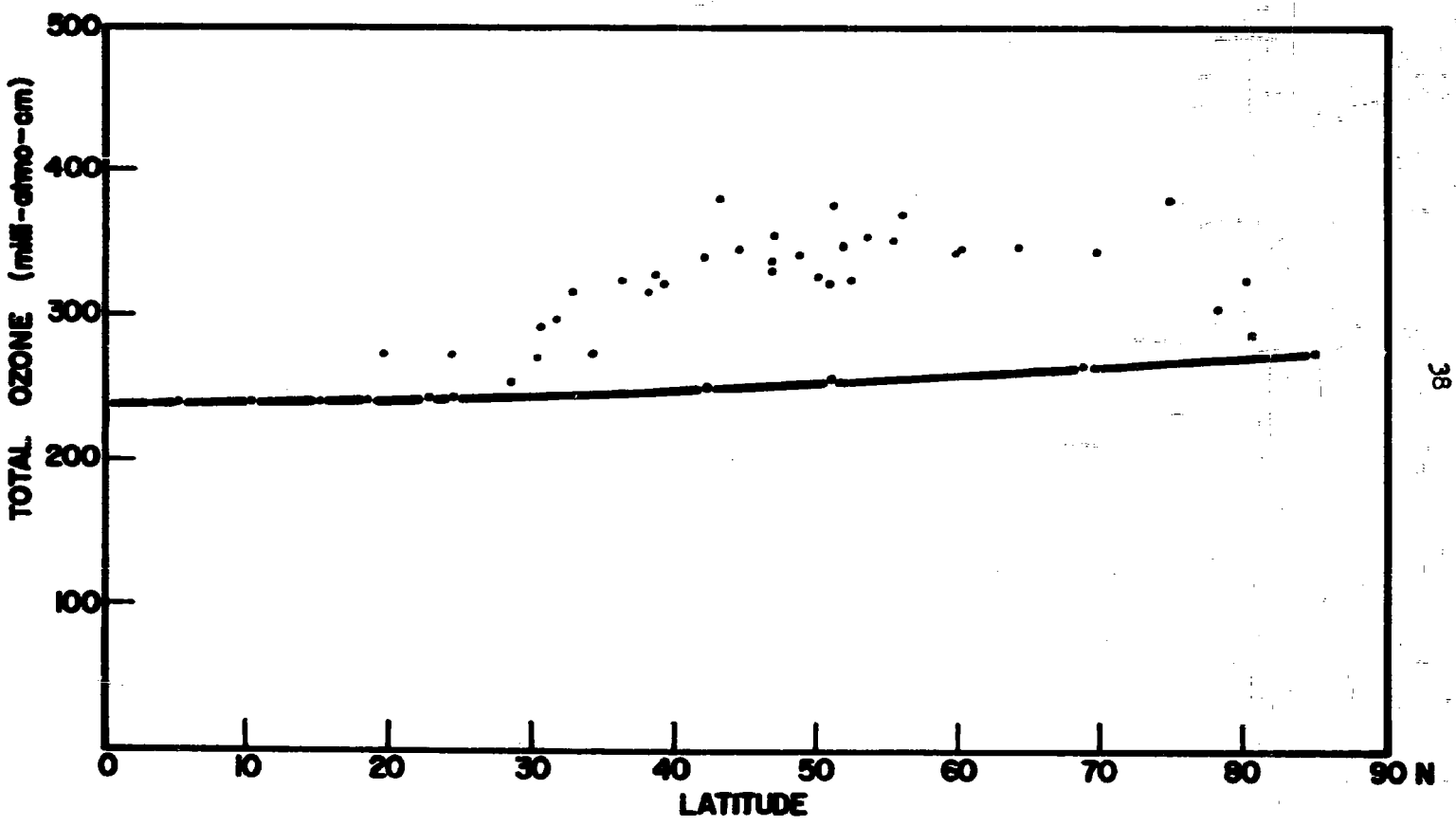

Fig. 9. The observed yearly mean total ozone (dots) vs latitude and the calculated values (solid curve) deduced from figure 8.

as:

$$(32) \qquad \frac{n_3(o,\lambda)\bar{v}f}{4} \int_o^{4H} e^{-z/H}\left[\int_o^z \frac{e^{-s/H}}{D}\,ds\right] dz$$

This term may be reduced to the approximate form

$$(33) \qquad \frac{n_3(o,\lambda)\bar{v}f}{4} \times \frac{3H^2}{\bar{D}}$$

where $\bar{D}$ is the average vertical diffusion coefficient over the range z = o to z = 4H. Cutting off the integral at z = 4H places the source at this altitude (about 27 km) and neglects the ozone above this altitude. Further, the observed yearly mean total ozone values would be accounted for by this term in a completely diffusion controlled theory. The yearly mean value of $\bar{D}$ required at 45° N is given, for example, by

$$(34) \qquad \frac{\bar{v}fn_3(o,\lambda)3H^2}{4\,\bar{D}} = 2.68 \times 10^{18} \text{ atoms/cm}^2 \times 3.5$$

Substituting the previously used sink strength and H = 7.5×10^5 cm

$$\bar{D} = \frac{6 \times 10^{10} \times 3 \times (7.5 \times 10^5)^2}{2.68 \times 10^{18} \times 3.5} \simeq 1.0 \times 10^4 \text{ cm}^2/\text{sec}$$

The mean values of $\bar{D}$ required as a function of latitude are given in Table II. The magnitude of $\bar{D}$ depends on the reciprocal of the yearly mean total ozone. Furthermore, the seasonal total ozone might similarly be explained by the seasonal variation in $\bar{D}$ given in Table II. According to this equilibrium theory, equation (26) would also yield the vertical eddy diffusivity from a measurement of the vertical profile. The eddy diffusivity would then be proportional to the reciprocal of the gradient of the mixing ratio, i.e.

$$(35) \qquad D = \frac{1/4n(o,\lambda)\bar{v}f}{n\frac{d\psi}{dz}} = \frac{1/4n(o,\lambda)\bar{v}f}{\frac{dn_3}{dz} + n_3\frac{Mg}{3RT_o}\left(\frac{T_o}{T}\right)\left[1 + \frac{R}{Mg}\frac{dT}{dz}\right]}$$

If n_3 is expressed in atoms/cm^3 and ΔT in °K, the above becomes for 5 km intervals

$$(36) \qquad \bar{D}_{5km}\left(\frac{cm^2}{sec}\right) = \frac{6 \times 10^{10}}{\Delta n_3 x 2x10^{-6} + n_3 x \left(\frac{T_o}{T}\right) 1.23x10^{-6}\left[1 + \frac{\Delta T}{170}\right]}$$

TABLE II

Computed Mean Vertical Diffusion Coefficient and Seasonal Variation Thereof

Latitude	0	10	20	30	40	50	60	70	80
$\bar{N}$ (milli-atmo-cm)	150	170	200	275	325	350	350	350	320
$\bar{D}(\lambda)$ cm^2 per sec	$2.5x10^4$	$2.2x10^4$	$1.9x10^4$	$1.4x10^4$	$1.2x10^4$	$1.1x10^4$	$1.1x10^4$	$1.1x10^4$	$1.2x10^4$
$\frac{\Delta\bar{D}(\lambda)}{\bar{D}(\lambda)}$	0	0	0	.1	.18	.28	.28	.30	.4

The values computed for flight 600 in figure 11 are tabulated in Table III. 5 km smoothed intervals were used in the calculations.

TABLE III

Computed Vertical Eddy Diffusivity for Flight 600

	0-5km	5-10km	10-15km	15-20km	20-25km
$\bar{D}_{5km}\left(\frac{cm^2}{sec}\right)$	1.8×10^5	8.6×10^4	2.6×10^4	6.3×10^3	1.2×10^4

The values obtained for $\bar{D}$ and $\bar{D}_{5km}$ are not unreasonable in view of the estimates of this quantity by Lettau (1951). Hence, the above calculations demonstrate the possibility that the majority of the ozone distribution may be diffusion controlled and that horizontal diffusion and advection may be unimportant for the gross features.

By far, the most significant feature of the ozone measurements is their correspondence with the temperature profile. This starts at the ground where it

is noticed that a decrease in ozone accompanies a temperature inversion near the surface. Moreover, the observed mixing ratio in the troposphere depends on the temperature lapse rate. The most pronounced variation in the ozone mixing ratio occurs at the tropopause. A well defined tropopause (abrupt change in the temperature lapse rate) is accompanied by a very sharp increase in the ozone mixing ratio. Likewise, where the temperature lapse rate changes gradually, the ozone indicates a poorly defined boundary between troposphere and stratosphere. Hence, the diffusive transport must be controlled to a large extent by the temperature distribution, and it is the semi-impermeable surface termed the tropopause which hinders any large quantity of ozone from entering the troposphere. This diffusion controlled process is advocated up to the level where photochemical time constants become comparable to the residence times consistent with the diffusive process. This level is probably in the neighborhood of 25 km in the vicinity of the observed ozone maximum which is lower than the photochemical maximum. This interplay between diffusive and photochemical processes is suggested as the cause for the observed ozone maximum being lower than the photochemical maximum. Furthermore, the concept of a net ozone production rate independent of the solar zenith angle and latitude is not inconsistent with the above ideas. The calculations of Craig (1950) show:

1. a maximum ozone concentration at 30 km for small zenith angles;

2. a rapid decrease of the ozone mixing ratio above the maximum with a scale height of roughly half of the atmospheric scale height. The second of these is characteristic of any photochemical equilibrium theory. The first is dependent upon assumptions regarding the oxygen absorption process. However, neither of the above are verified by the observations in this work. With a large diffusion coefficient and with the rapid decrease of the ozone mixing ratio above the maximum required by photochemical equilibrium, ozone would be transported upward where it would be photochemically destroyed. This process

would lower the maximum and increase the ozone scale height above the maximum. For large solar zenith angles, however, the photochemical scale height is approximately that of the atmosphere, greatly reducing or preventing upward transport. Hence, it is possible that large solar zenith angles yield no less ozone above the maximum than small zenith angles under identical temperature and diffusion conditions. To reverse the effect under identical diffusion conditions would be possible since, as was outlined earlier in the section on photochemical equilibrium, the k factor is very temperature dependent and is such as to increase the ozone concentration at high levels in the winter or early spring and to decrease it in the late summer. The observations shown in figures 10, 11, 12 and 13 support this. Moreover, if the absorption coefficient of oxygen is pressure dependent, the above argument would lead to a broad maximum for large solar zenith angles and a more pronounced maximum for small zenith angles. This also is suggested by the data in figures 10, 11, 12, and 14. It is reasonable to expect, then, that the observed maximum exists at a level where the photochemical time constant and the residence time for the transport process are the same. This level may change with the season. The data in figures 10, 11, 12, and 13 suggest that this level is higher in the spring (broad maximum) than it is in the summer (sharp maximum). This is consistent with a larger photochemical time constant at large solar zenith angles. However, it is mandatory that more observations be made to test these ideas.

The vertical profiles of the atmospheric ozone distribution shown in figures 10, 11, 12, and 13 are unique in two respects:

1. They are among the first of such measurements which yield structure in the vertical ozone distribution heretofore unresolved while at the same time providing a measure of the integrated ozone between ground level and balloon altitudes.

2. They furnish measurements of ozone in a manner which is com-

pletely different from other techniques.

The chemiluminescent ozone detector will easily resolve structure in the vertical distribution which cannot be shown in figures 10, 11, 12, and 13. This feature is a prerequisite in the study of advective processes. It has been shown (Kroening and Ney, 1962) that ozone structures with vertical dimensions of the order of 1 km exist in the troposphere. These thin stable laminae, termed ozone 'rivers,' are attributed to the vertical advection of air between the stratosphere and the troposphere and thus retain an ozone concentration characteristic of their origin. These ozone rivers are shown in figure 10 and 11 and appear to be characteristic of the late summer soundings (July and August). The distinguishing feature between an ozone river and a diffusive maximum has been assumed to be in the nature of the mixing ratio above the maximum. In the formation of a diffusive maximum, the mixing ratio cannot decrease above the maximum. In the case of advection, this criterion need not be satisfied and most likely will not. For example, the maxima at 145 mb in figure 13 and 165 mb in figure 10 are indicative of an advective process, that is, an ozone river. In neither of these cases is it clear what fraction of the advection is vertical and what fraction is horizontal. Most likely it is a combination of both. The temperature profile associated with these rivers, however, suggests downward transport as the major advection. Certainly, soundings on a synoptic basis or a vehicle navigating on these rivers would provide the answer. It has been shown (Ney and Kroening, 1961) that these ozone rivers can only persist in the case of continued descending motion and it was this idea that led to their naming. Any ascending lamina will be characterized by a low ozone concentration and much larger vertical dimensions.

The three balloon flights (593, 600, 596), besides providing the vertical ozone distribution, were maintained at high altitude through sunrise in order to determine the diurnal ozone variation at high altitude. The resutls obtained

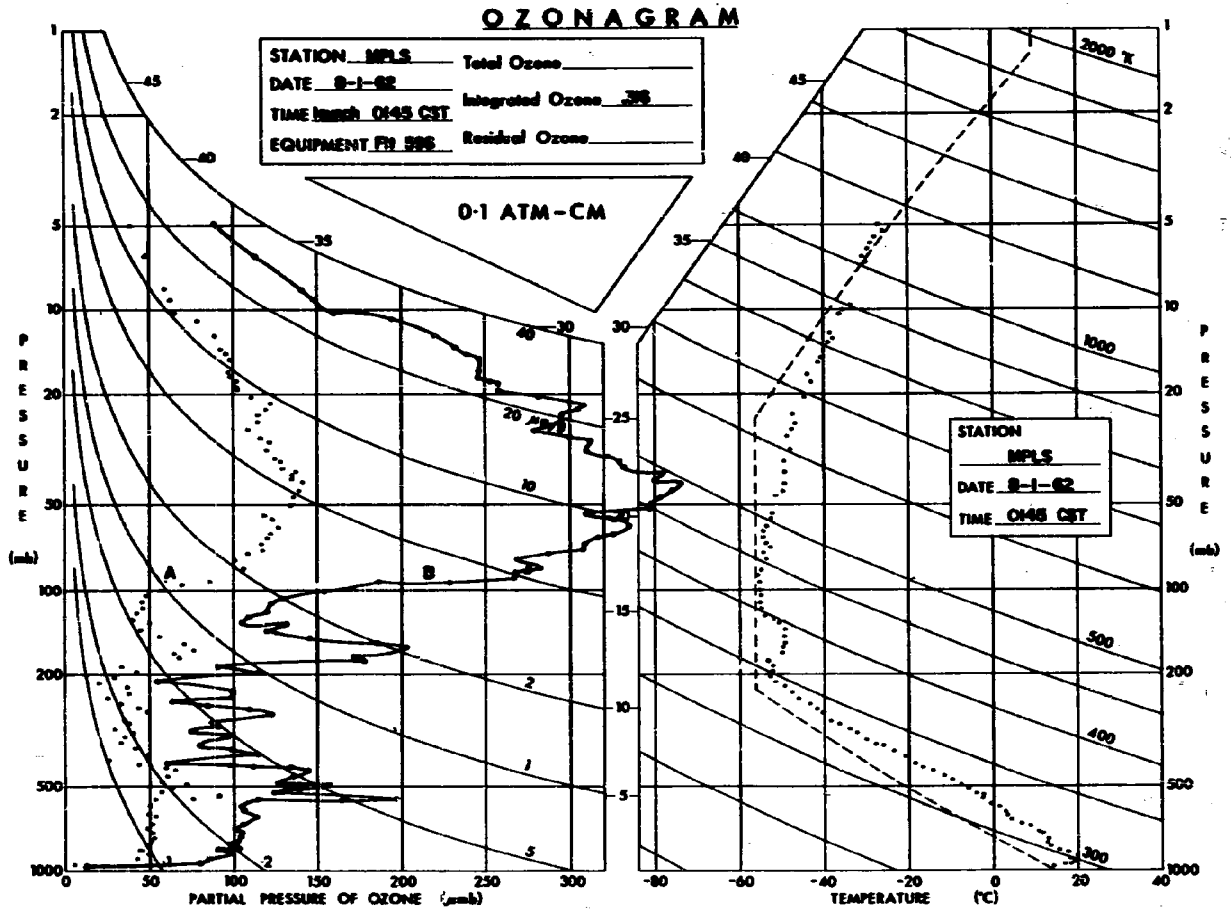

Fig. 10. Vertical ozone distribution and temperature profile over Minneapolis on Aug. 1, 1962. Curve A is the partial pressure of O_3 in μmb, Curve B is the ozone density in $\mu g/m^3$ with same scale as A.

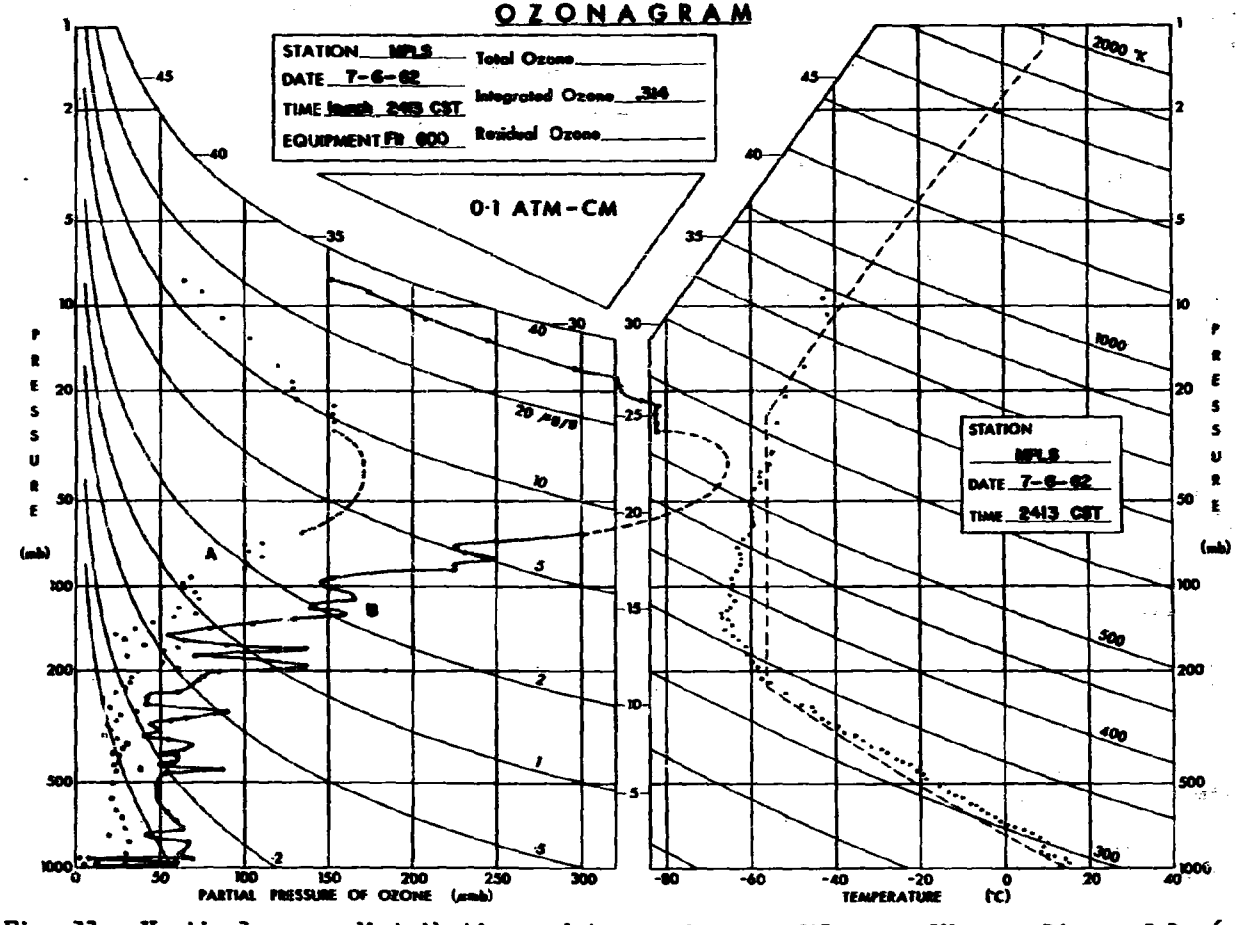

Fig. 11. Vertical ozone distribution and temperature profile over Minneapolis on July 6, 1962. Curve A is the partial pressure of O_3 in umb, Curve B is the ozone density in $\mu g/m^3$ with same scale as A.

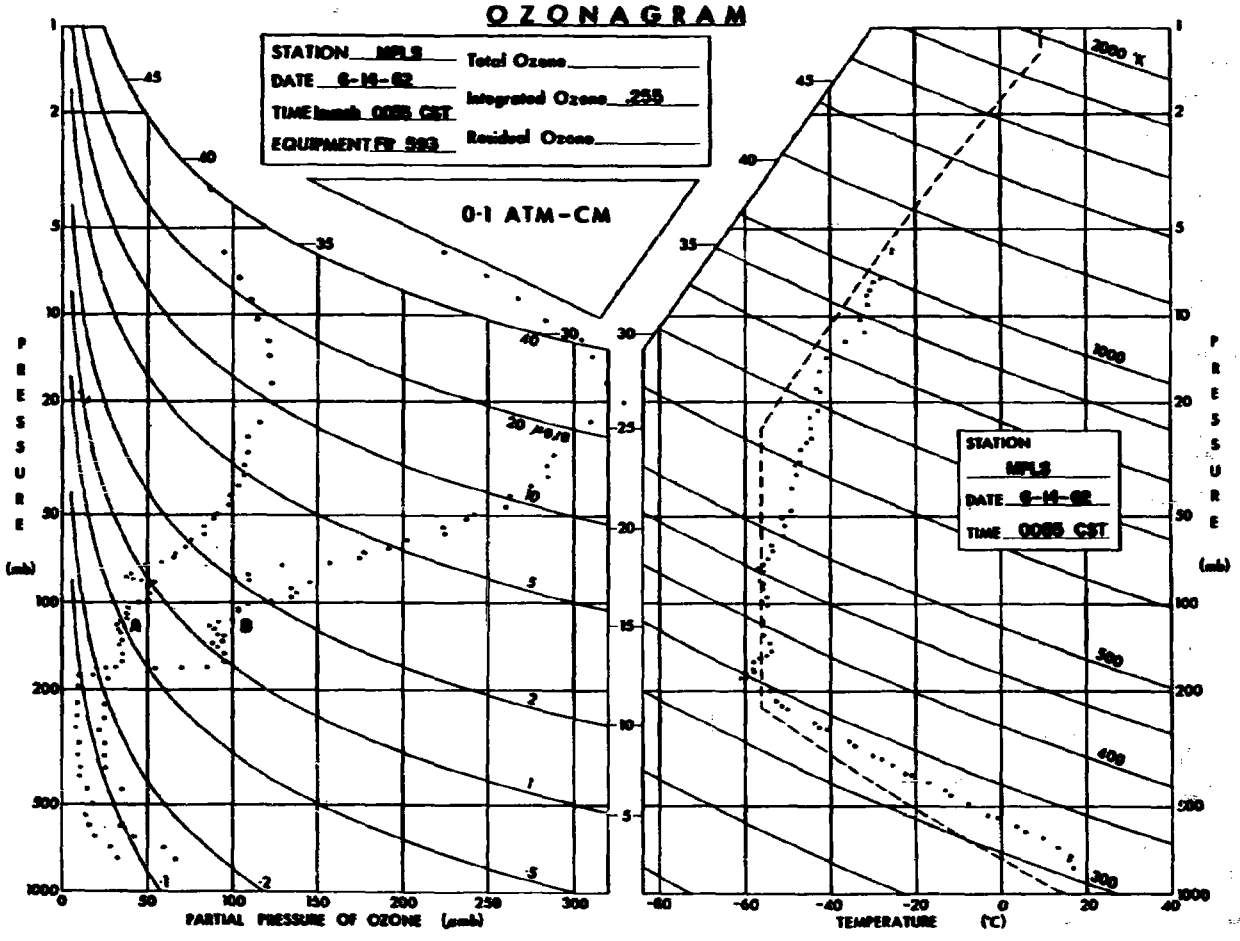

Fig. 12. Vertical ozone distribution and temperature profile over Minneapolis on June 14, 1962. Curve A is the partial pressure of O_3 in μmb. Curve B is the ozone density in $\mu g/m^3$ with same scale as A.

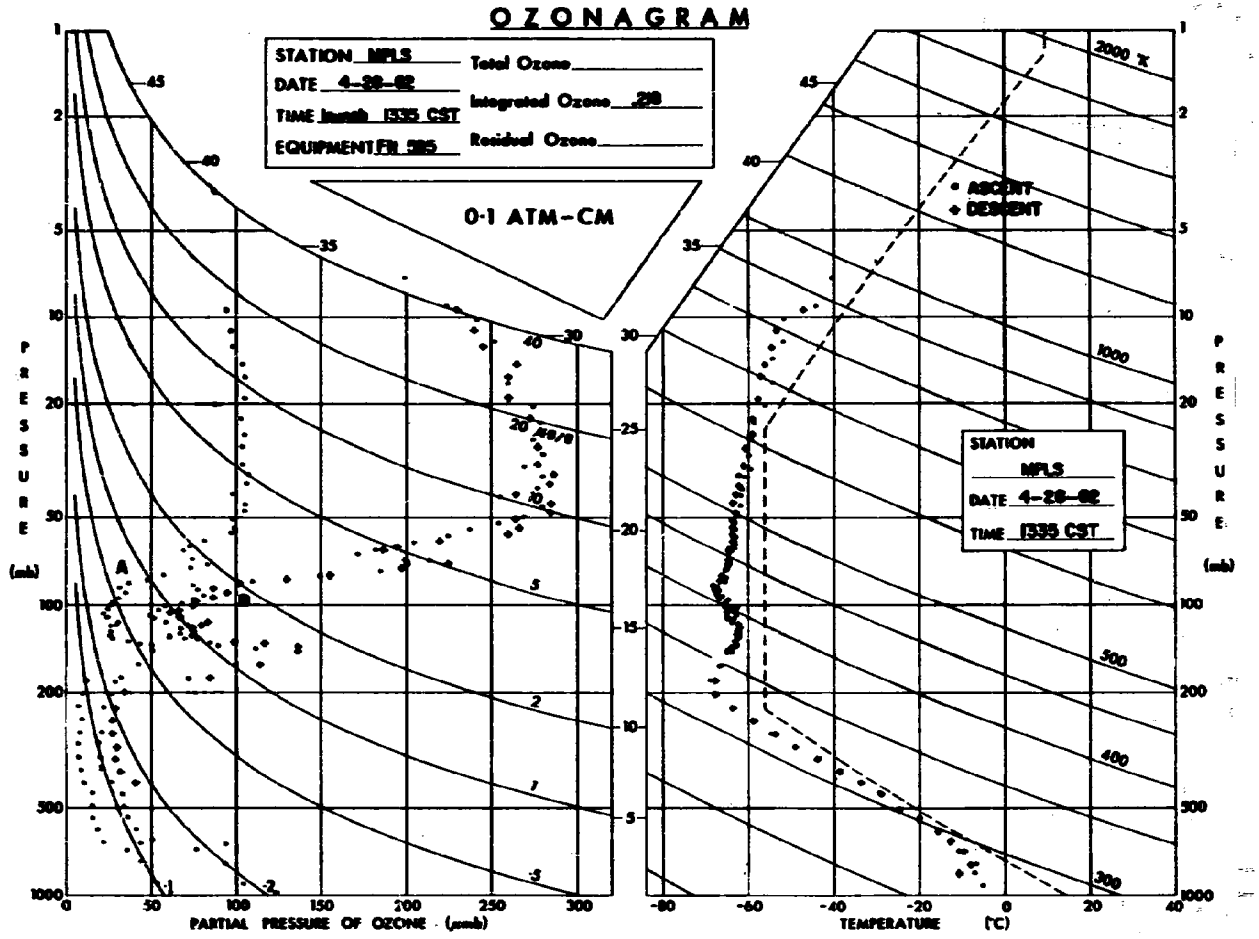

Fig. 13. Vertical ozone distribution and temperature profile over Minneapolis on April 28, 1962. Curve A is the partial pressure of O_3 in μmb. Curve B is the ozone density in $\mu g/m^3$ with same scale as A.

are shown in figure 14, with S.R. indicating sunrise at ground level. Because of the lack of consistency between the three soundings, it is unclear whether the data represent ambient conditions. Balloon and gondola effects cannot be ruled out. There is a tendency for a downward flow of air around the balloon at night and the opposite circulation after sunrise. This could explain the higher readings after sunrise. Certainly, the diurnal variation is less than 30%. More refined experiments are evidently needed.

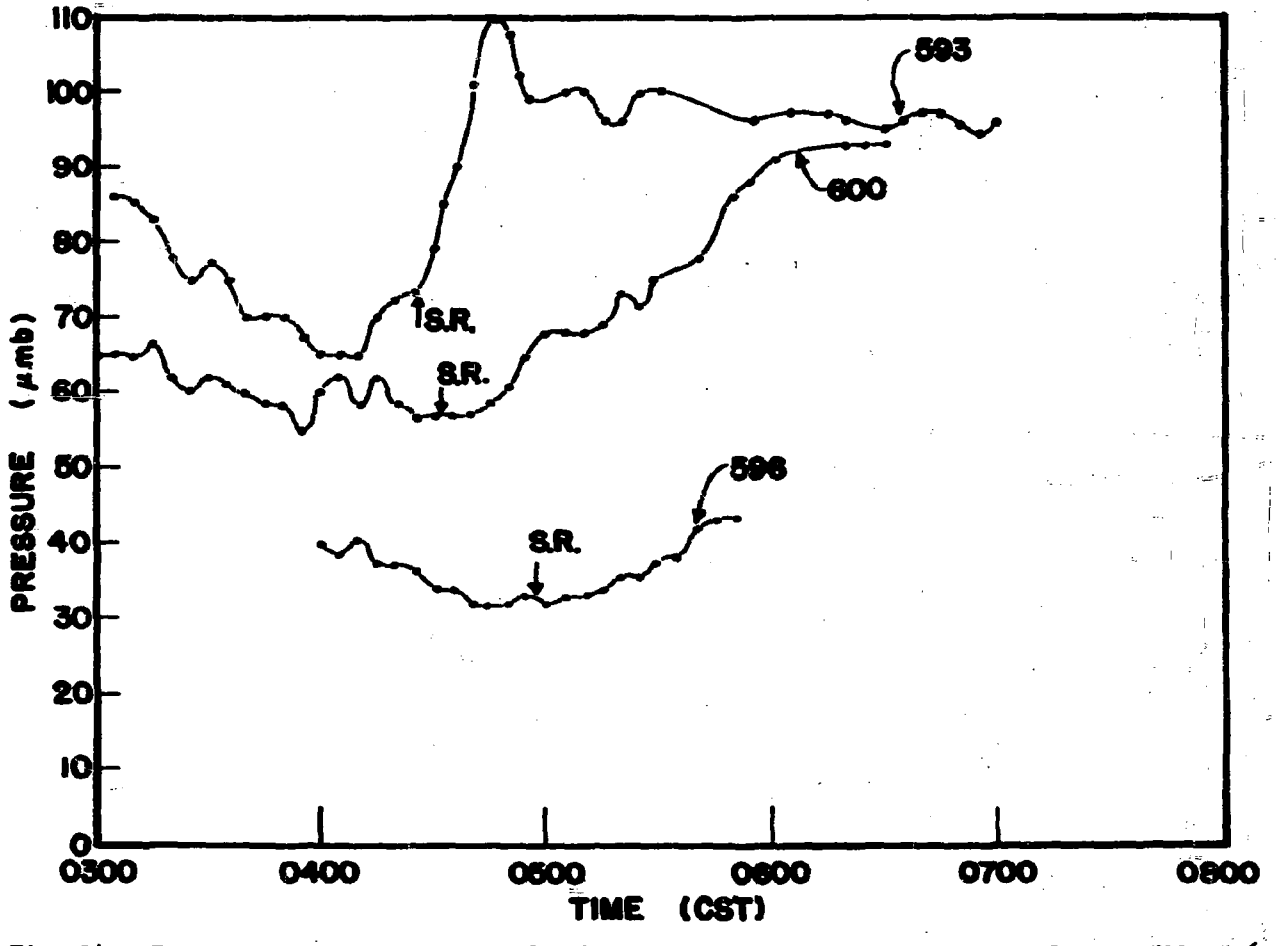

Fig. 14. The partial pressure of O_3 (μmb) vs time at ceiling altitude of flights 593, 596 and 600. S.R. indicates ground sunrise.

PRODUCTION OF OZONE

The source of ozone as outlined earlier in this writing was taken as that occuring in the high atmosphere from solar energy. It appears, however, that this cannot be taken as the only significant source (Kroening and Ney). Electrical discharge phenomena apparently involve enough energy dissipation with a high enough efficiency to compensate for the ozone removed from the atmosphere at the ground. Cauer (1951) gives strong evidence for the production of ozone in regions of high electric fields without the spark discharge. Regener (1943) has reported observations of high ozone levels under thunderstorm conditions at cloud levels in the troposphere. Kroening and Ney (1962) have measured an efficiency factor for ozone production by a C_o^{60} radioactive source and arrive at the value .03 atoms of ozone per electron volt dissipated in the air. This is about one ozone atom for every ion pair. A nearly identical efficiency factor is obtained in the laboratory controlled electrical discharge in air. It is thought that this is more than coincidental and suggests the conclusion that this efficiency factor applies to any very energetic process. In light of the possibility of the production of large amounts of ozone by electrical discharges, experiments should undoubtedly be carried out to check this. Measurements around thunderstorms should be made aloft. Surface measurements are likely to be obscured. However, it should be mentioned that during a large thunderstorm occuring on 5/22/62 and 5/23/62, a very large increase in ozone arriving at the surface was recorded at Minneapolis. The ozone reached a level slightly in access of 10 pphm by volume while the average for an 18-hour period was 6 pphm, almost twice the mean surface level. In view of the data available at present concerning the production of ozone in electric discharges, it appears that it cannot be neglected.

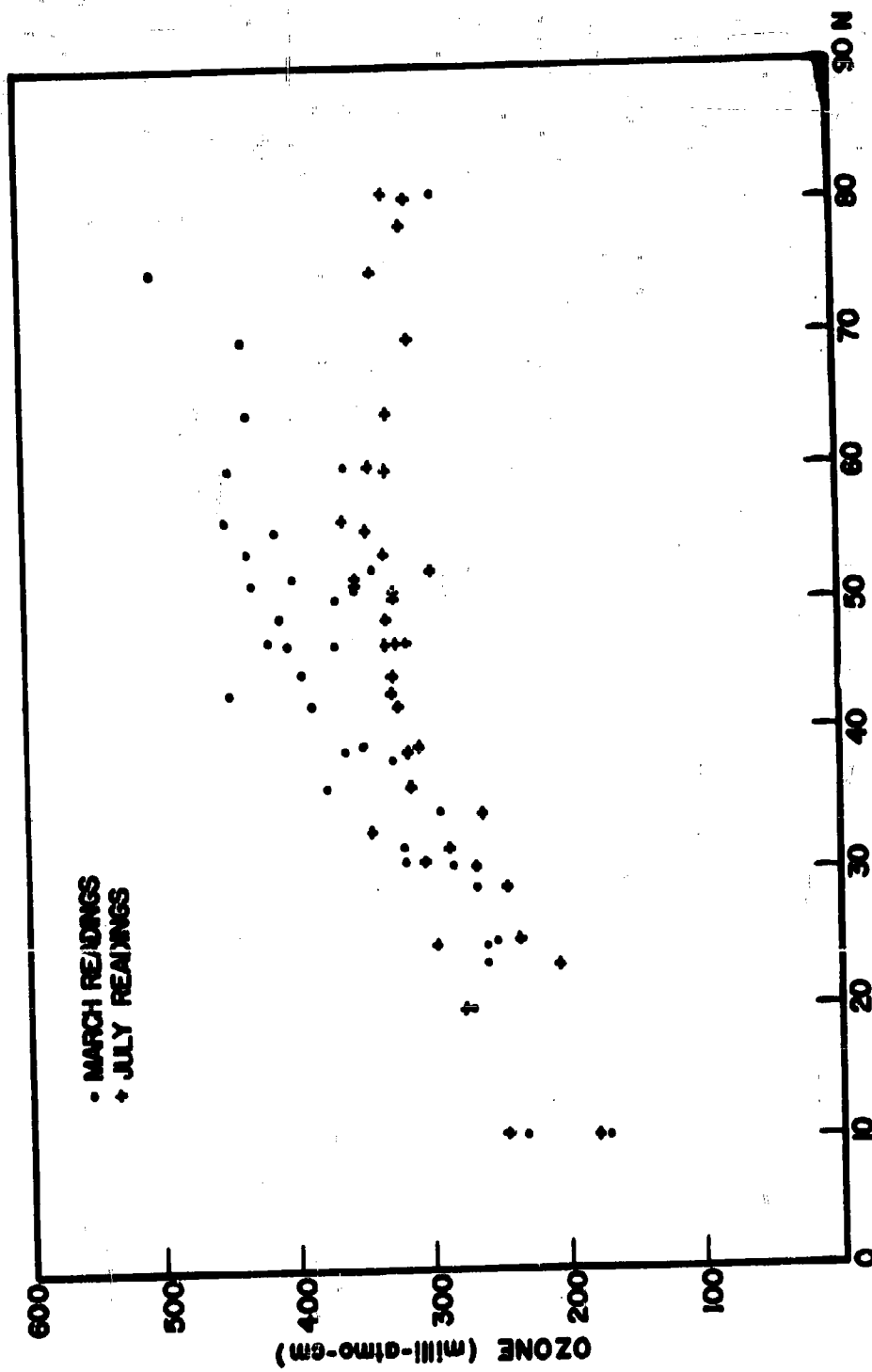

Fig. 15. The observed monthly mean total ozone vs latitude for March and July.

SUMMARY

1. A chemiluminescent ozone detector is described which allows detailed measurements of the atmospheric ozone concentration.

2. There is a diurnal variation of the atmospheric ozone concentration 1 m above the ground on almost all days but to a varying degree.

3. An average relationship between the surface level wind speed and the ozone concentration 1 m above the ground at Minneapolis is given.

4. The strength of the ozone sink at Minneapolis is given and from this the general properties of the ground level sink are deduced. A definite latitudinal variation of the tropospheric ozone concentration results with more ozone at higher latitudes. The effect of the ground level sink on the total ozone value, however, is shown to be negligible if an allowance is made for the solar insolation available at the top of the atmosphere.

5. Theoretical and experimental evidence for the formation of a low level ozone maximum in the troposphere is given.

6. A completely diffusion-controlled model of the vertical ozone distribution is presented and the appropriate values for the vertical eddy diffusivity are given.

7. The existence of thin stable lamina of ozone, termed ozone 'rivers,' is demonstrated. These rivers descend through the atmosphere and retain an ozone concentration characteristic of their origin.

8. It is pointed out that the production of ozone by electrical discharges within the atmosphere cannot be ruled as insignificant.

APPENDIX I

Procedure for the Chemical Determination of Ozone Concentrations

Reagents:

Buffer solutions - 1.8 g of $Na_2 HPO_4$ y + 1.7 g of KH_2PO_4 in 1 liter of water.

.0001N00 N or .00100N KIO_3 - .0214 g or .214 g or KIO_3 in 1 liter of water.

2 N sulfuric acid.

KI free from iodate.

Amperometric probe, magnetic stirrer, 5 ml buret graduated, Flowmeter, bubbler bottles.

Procedure:

Place 70 ml of buffer solution, 1 g of KI and 5 ml of $Na_2S_2O_3$ (measured with 5 ml pipette) solution in each of the two bubbler bottles. Pass ozone through at the rate of 500 cc per minute for about 20 minutes. Add 10 ml $2N\text{-}H_2SO_4$. Titrate with standardized KIO_3 solution from buret using an amperometric probe made of silver and gold (anode and cathode respectively).

Caution should be taken to cleanse all apparatus before the sample is taken. Distilled water should be used for all solutions. A dry run is generally made first (without ozone) to test the stability of $Na_2S_2O_3$ during the sampling time. Care must be taken not to use all of the $Na_2S_2O_3$ during the ozone determination or a rerun with more $Na_2S_2O_3$ or less time is required. A blank a day is a good idea to keep the decomposition of the $Na_2S_2O_3$ solution in view. The bubblers used should be of the large hole type. Fine hole bubbler bottles decompose

ozone. The plumbing should be all glass and plastic. No stopcock grease should be used on fittings. In all of the calibrations, tank oxygen was used.

APPENDIX II

(Insolation Langleys/Day)

Month	J	F	M	A	M	J	J	A	S	O	N	D
Latitude												
0 - 10	800	850	860	850	840	830	840	850	860	840	820	800
12 - 20	710	760	820	890	900	890	900	890	850	800	720	690
20 - 30	590	680	800	880	910	910	910	890	830	710	610	550
30 - 40	450	550	700	850	910	920	910	880	750	600	470	800
40 - 50	300	410	620	790	900	960	930	820	670	480	330	250
50 - 60	150	280	490	720	900	970	920	770	550	350	190	120
60 - 70	45	145	350	590	860	990	910	700	440	200	70	20
70 - 80	0	0	210	500	860	1010	950	650	300	75	10	0
80 - 90	0	0	50	500	850	1010	960	610	180	20	0	0

APPENDIX III

Surface Temperature -- London's data			
Latitude	Yearly Mean Temp (°C)	Winter Temp (°C)	Summer Temp (°C)
0 - 10	26.8	27.3	27.3
0 - 20	26.8	24.7	27.9
20 - 30	23.7	19.4	26.9
30 - 40	17.4	10.5	23.2
40 - 50	9.5	.4	18.3
50 - 60	2.6	-8.5	13.3
60 - 70	-5.3	-18.9	9.6
70 - 80	-11.3	-25.1	3.4
80 - 90	-16.4	-30.2	.4

OZONE BIBLIOGRAPHY

Bernanose, A.J., and Réné, M.G., Ozone Chemistry and Technology, American Chemical Society, Washington D.C., pp. 7-12, 1959.

Biswas J., and Dhar, N., Chemiluminescenz bei der Oxydation von Farbestoffen durch Ozon, Z. Anorg. Chem. 173, pp. 125-136, 1928.

Briner, E., Notice sur une oxydation fortement luminescente provoquée par l'ozone, Helv. Chim. Acta,23, p. 320, 1940.

Ibid., Ozone Chemistry and Technology, American Chemical Society, Washington D.C., pp. 1-6, 1959.

Cauer, H., Compendium of Meteorology, American Meteorological Society, Boston, Mass., ed. T.F. Malone, pp. 1126-1136, 1951.

Chapman, S., On the Annual variation of upper-atmospheric ozone, Phil. Mag., 10, pp. 345-352, 1930.

Ibid., On Ozone and atomic oxygen in the upper atmosphere, Phil. Mag., 10, pp. 369-383, 1930.

Ibid., The photochemistry of atmospheric oxygen, Rep. Prog. Phys., London, The Physical Society, 9, pp. 92-100, 1943.

Ibid., Physics and Chemistry of the Upper Atmosphere (Lecture Notes), Dept. of Physics, State University of Iowa, Iowa City, p. 157, 1955.

Craig, R.A., The Observations and Photochemistry of Atmospheric Ozone and their Meteorological Significance, Meteorlogical Monographs, Vol. I, No. 2, 1950.

Dhar, N., The Chemical Action of Light, Blackie and Son Limited, Toronto, pp. 350-363, 1931.

Eucken, A., and Patat. F., Die Temperaturabhaengigkeit der Photochemischen Ozonbildung, Z. Phys. Chem., B 33, pp. 459-474, 1936.

Fritz, S., Compendium of Meteorology, American Meteorological Society, Boston, Mass., ed. T.F. Malone, pp. 1126-1136, 1951.

Gergen, J.L., Ozone, Summary Report--Atmospheric Physics Program, University of Minnesota, Minneapolis, Nonr-710 (22), p. 39, 1959 and 1960.

Goldberg, L., The Earth as a Planet, University of Chicago Press, Chicago, Ill., G.P. Kuiper, ed., p. 457, 1953.

Gotz, F.W., Compendium of Meteorology, American Meteorological Society, Boston, Mass., ed. T.F. Malone, pp. 275-289, 1951.

Harvey, E.N., Luminescence during electrolysis, J. Phys. Chem., 33, pp. 1456-1459, 1929.

Heilpern, W., Die Absorption des Lichtes durch Sauerstoff bei der Wellenlaenge λ = 2144 A° in Abhaengigkeit vom Druck, Hlv. Phys. Acta, 14, 329-354, 1941.

Ibid., Die Absorption des Lichtes durch Sauerstoff im Wellenlaengen bereich λ = 2100 bis λ = 2400 A° in Abhaengigkeit vom Druck, Helv. Phys. Acta, 19, pp. 245-265, 1946.

Iler, R.K., The Colloid Chemistry of Silica and Silicates, Cornell University Press, Ithaca, N.Y., p. 170, 1955.

Kautsky, H., and Zocher, H., Uebereinige ungesaettigte Siliciumverbindungen, Z. Anorg. Che., 117, p. 209, 1921.

Ibid., Chemiluminescence, Trans. Faraday Society, 1925 (advance proof), Chemical Abstracts, 20, p. 551, 1926.

Kearney, Phil Mag. 42, p. 48, 1924.

Kroening, J.L., and Ney, E.P., Atmospheric ozone, Journal Geophys. Res., 67, pp. 1867-1875, 1962.

Lettau, H., Compendium of Meteorology, American Meteorological Society, Boston, Mass., ed. T.F. Malone, pp. 320-333, 1951.

London, J., A study of the atmospheric heat balance, Dept. of Meteorology and Ozeanography, New York University, prepared for Air Force Cambridge Research Center, AF CRC-TR-57-287, AD 117227, 1957.

Ney, E.P., and Kroening, J.L., Atmospheric ozone, Technical Report No. AP-18, Atmospheric Physics Program, University of Minnesota, 1961.

Regener, E., Ozonschicht und Atmosphaerische Turbulenz, Meteor. Z., 60, pp. 253-269, 1943.

Regener, V.H., On a sensitive method for the recording of atmospheric ozone, J. of Geophys. Res., 65, pp. 3975-3977, 1960.

Wadelin, C.W., Determination of O_3 and other oxidants in air, Anal. Chem., 21, pp. 441-442, 1957.

Wilhelmsen, P.C., Lumry, R., and Eyring, H., The Luminescence of Biological Systems, American Association for the Advancement of Science, Johnson, F.A., ed., pp. 75-98, 1955.

Wulf, D.R., A Theory of the ozone of the lower atmosphere and its relation to the general problem of atmospheric ozone, Phys. Rev., 41, pp. 375-376, 1932.

Ibid., Steady states produced by radiation with application to the distribution of atmospheric ozone. Phil. Mag., 17, pp. 251-263, 1934.

Wulf, O.R., and Deming, L.D., The Theoretical calculation of the distribution of photochemically-formed ozone in the atmosphere, Terr. Mag., 41, pp. 299-310, 1936.

Ibid., The Effect of visible solar radiation on the calculated distribution of atmospheric ozone, Terr. Mag., 41, pp. 375-378, 1936.

Ibid., The Distribution of atmospheric ozone in equilibrium with solar radiation and the rate of maintenance of the distribution, Terr. Mag., 42, pp. 195-202, 1937.

SMALL ATMOSPHERIC IONS

Introduction

The equilibrium theory of small atmospheric ions and the technique of measuring them has been outlined elsewhere (Kroening, 1959). The theory involves the following equation:

$$(1) \qquad \frac{dn}{dt} = q - \alpha n^2 - \sum_R \beta(R)\, N\,(R)\, n$$

where n is the number density of small ions, N is the number density of large nuclei, charged or uncharged, q is the production rate of small ions, α is the Thomson volume recombination coefficient and β is the related coefficient for recombination between small ions and nuclei. The production rate is usually attributed to cosmic rays. The last term on the right side of the equation (1) has been neglected or deemed unimportant in the equilibrium theory above the exchange layer. It has been neglected largely because an understanding of the small ion - large nuclei interaction is lacking except at ground levels, and even here the value of β is not a well defined quantity. For example, the values of β reported vary from $.4 \times 10^{-6} cm^3/sec$ up to $8 \times 10^{-6} cm^3/sec$. An average value of $2 \times 10^{-6} cm^3/sec$ at N T P is normally adopted. Furthermore, it is the opinion of the author that any conductivity measurements or ion density measurements made at heights greater than 25 km in the daytime are subject to serious error unless special precautions have been taken to eliminate photoelectron ejection from the collector. This effect has been observed on every daytime flight made by the author and if not eliminated obscures the effect of large nuclei (Kroening, 1960). Mention of this in the literature has been made only by the author. Yet, daytime measurements which are likely in error are

taken as representative of ambient conditions. Moreover, the conductivity measurements are not directly applicable to the equilibrium theory since these measurements have the ionic mobility folded into them. The ion density measurements reported in this writing and elsewhere were made at night to eliminate these problems. Consequently, it is advocated that they are representative of ambient conditions in the high atmosphere. Daytime measurements of the conductivity at high altitude which are explained solely by small ion recombination must be judged as fictitious, since all of the authors measurements, except one, show a deficit in the small ion density at high altitudes. It is felt that this can only be explained by the presence of Aitken nuclei at high altitude.

THEORY AND MEASUREMENTS

The small ion recombination process has been studied considerably and the recombination coefficient governing it has been given by Thomson. Very little is known concerning the small ion - large nuclei recombination process. Hence, in this part of the dissertation, an attempt will be made to describe the importance of the last term on the right of equation (1), especially at high altitudes.

Measurements of q for the appropriate latitude (45° N) as well as a graph of α have been given elsewhere (Kroening, 1959). In an attempt to estimate β a simple method of arriving at the value of α will be presented. The attractive force between positive and negative singly charged ions is e^2/r^2, whereas the potential between the two is e^2/r. For the two ions to recombine requires that the relative kinetic energy is such as to allow a closed orbit of one about the other. In a gas at temperature T, this requires

$$\frac{e^2}{r} \geq \frac{3kT}{2} \tag{2}$$

Hence, they must approach at least as close as

$$r_o = \frac{2e^2}{3kT} \tag{3}$$

Furthermore, during the time that the two ions satisfy equation (2), a collision of either of the two ions with an air molecule which reduces the relative kinetic energy by an amount kT must occur. Then recombination is effected. These are the fundamental assumptions made by Thomson. If the probability of the collision of the ions with the neutral air molecules while $r \leq r_o$ are s_+ and s_-, then the recombination rate when $n_+ = n_- = n$ will be

$$\bar{v}\pi r_o^2 n^2 (s_+ + s_- - s_+ s_-)$$

Hence

$$\alpha = \bar{v}\pi r_o(s_+ + s_- - s_+s_-) \tag{4}$$

If we write s_+ and s_- as

$$s_+ = 1 - e^{-2r_o/L_+}$$

$$s_- = 1 - e^{-r_o/L_-} \tag{5}$$

$$L_+ \simeq L_- = L \text{ mean free path length}$$

Then for high pressures

$$s_+ + s_- - s_+s_- = 1$$

$$\alpha = \bar{v}\pi r_o^2 \tag{6}$$

and for low pressures

$$s_+ + s_- - s_+s_- \simeq \frac{4r_o}{L}$$

$$\alpha \simeq 4\frac{r_o}{L}\bar{v}\pi r_o^2 \tag{7}$$

Consider the value of r_o

$$r_o = 4.05 \times 10^{-6}\left(\frac{273}{T}\right) \text{ cm} \tag{8}$$

Hence, for the large nuclei ($R \gg r_o$) the value of the recombination coefficient given by

$$\beta = \bar{v}\pi R^2 \tag{9}$$

is suggested. It will be assumed that equation (9) gives the small ion - large nuclei recombination coefficient.

For nuclei with radii $R \ll r_o$ a combination of the Thomson coefficient and the above is necessary. For equilibrium conditions, equation (1) then becomes

$$\Sigma\beta N = \left[\frac{q}{\alpha n^2} - 1\right]\alpha n = \left[\frac{n_o^2}{n^2} - 1\right]\alpha n \tag{10}$$

or

$$\Sigma\beta N = \frac{q}{n} \quad \text{if } \alpha n \text{ is small.} \tag{11}$$

where n_o is the equilibrium number density if no Aitken nuclei are present.

Thus, the term $\Sigma\beta N$ is important when any deficit in the small ion density

occurs. Likewise, any excess observed in the small ion density is to be attributed to sources other than cosmic radiation. The possibility of variations occuring in the cosmic ray production are remote at the altitudes considered except on special occasions (solar flares etc.). Since the advent of nuclear testing and in view of the residence time of radioactive material near and above the tropopause (List, 1962), an excess of small ions is expected and is observed at the base of the stratosphere.

Consider the data of flight 587, figure 16, tabulated in Table IV. If one divides the term $\Sigma\beta N$ by the mean ionic velocity one obtains the geometrical cross sectional area of the nuclei per cm^3 if they have radii $R \simeq r_o$. If the nuclei in the main have radii $R << r_o$, the area obtained is fictitious. It should be noticed though that as far as recombination is concerned the larger nuclei are weighted according to their cross sectional area. Moreover, the large nuclei ($R \gtrsim r_o$) become increasingly more important at lower pressures since β is not pressure dependent whereas α is proportional to the pressure. The nuclei ($R < r_o$) are associated with a recombination coefficient which is not nearly as pressure dependent as α save for very small R. The 'excess' entries in Table IV under $\Sigma\beta N$ arise since here $n > n_o$. In this region, it must be assumed that cosmic rays are not the only important production factor. The quantity of radioactive material available for small ion production has been measured by Machta and List (1959) and List (1962).

One can at best say that this is a variable quantity. But to demonstrate that it is present in sufficient quantity to affect the ion density note figure 17. On this flight there is a pronounced layer with high ion density restricted to the pressure range 150 mb - 110 mb. This layer is probably in advective motion descending through the stratosphere. The descending motion is suggested by the temperature profile associated with the ion peak. The ion density in this layer approaches twice the level outside the layer. An additional produc-

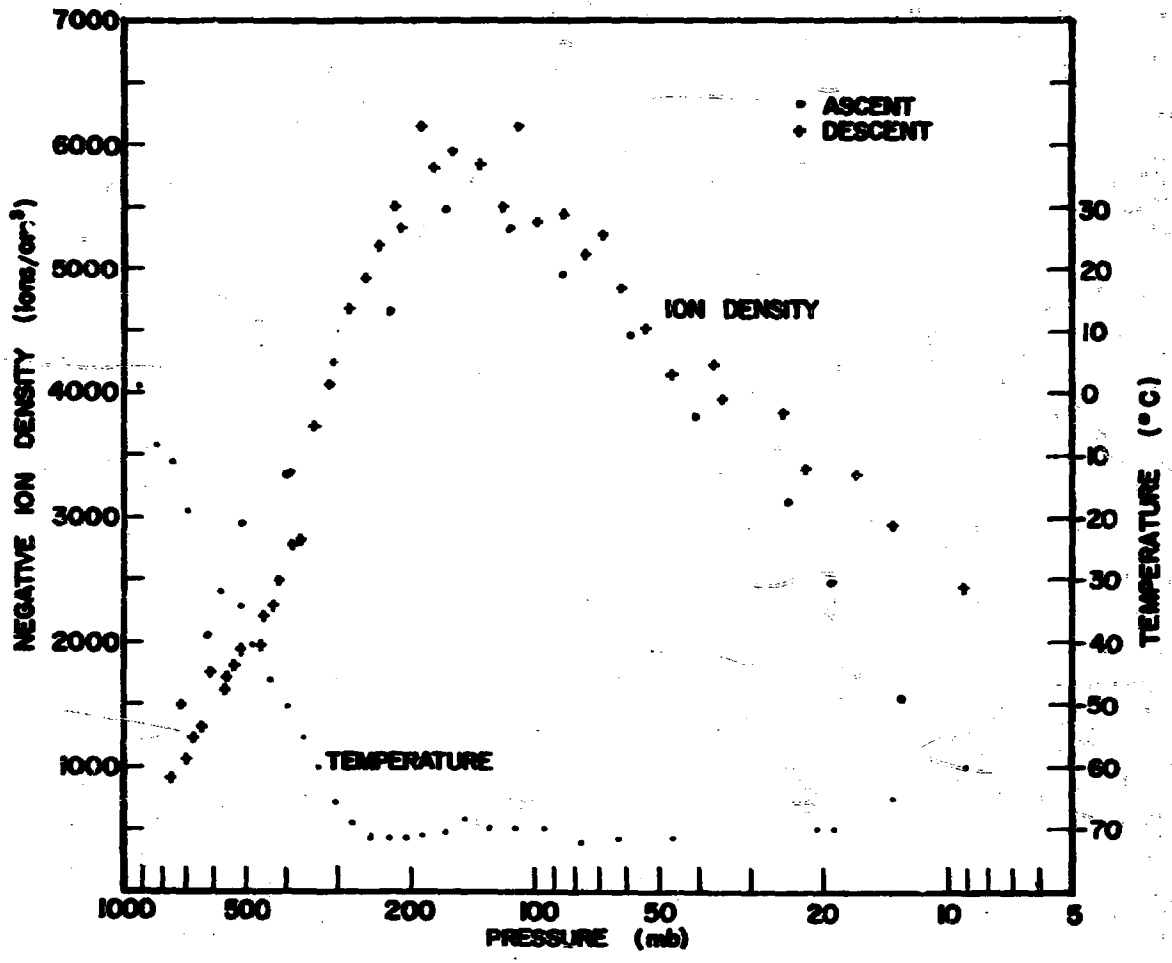

Fig. 16. The ion density and temperature profiles of flight 587 for May 2, 1962, over Minneapolis.

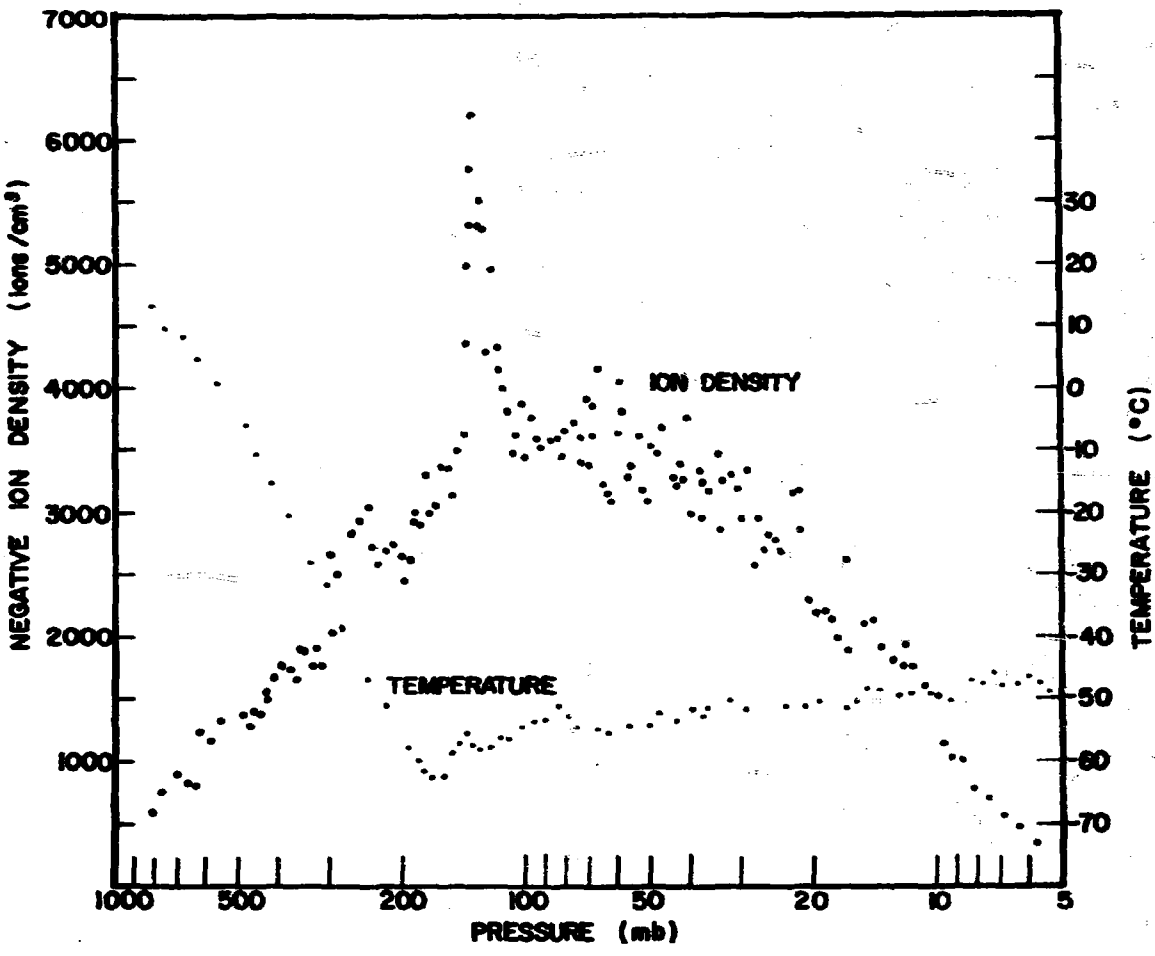

Fig. 17. The ion density and temperature profiles of flight 562 for October 30, 1961, over Minneapolis.

TABLE IV

p(mb)	$n(\frac{ions}{cm^3})$	$n_o(\frac{ions}{cm^3})$	$\alpha\ (\frac{cm^3}{sec})$	$\beta N(\frac{ions}{sec})$
800	850	980	2.1×10^{-6}	$.58 \times 10^{-3}$
500	2500	2000	2.1	excess
300	4300	3220	2.5	excess
150	5800	4160	1.9	excess
70	5000	4390	1.1	excess
30	3750	4120	.53	$.46 \times 10^{-3}$
10	2500	3780	.18	$.90 \times 10^{-3}$

tion rate which is approximately twice that of cosmic rays must be assumed. This layer is analogous to the ozone rivers discussed in the previous section on ozone.

The lower limit of the particle size responsible for the deficit of small ions at high altitude is partly determined by the collector used in the measurements. Since the collector will saturate on ions with a mobility of $1\ \frac{cm^2}{volt\ sec}$ at N T P, it will saturate w.r.t. ions of about 1/100 of this mobility at 10 mb. The mobility of large ions at the surface is about $5 \times 10^{-4}\ \frac{cm^2}{volt\ sec}$. These have a radius of about 5×10^{-6} cm and will not be collected at high altitude. The intermediate ions have a mobility of about $7 \times 10^{-2}\ \frac{cm^2}{volt\ sec}$ at N T P and a radius of about 4×10^{-7} cm. These will be collected at high altitudes. Hence, it appears that the particles must be on the order of 10^{-6} cm radius or larger.

To get an idea of the magnitude of the nuclei number density required to explain the observations, consider the deficit present at 10 mb in flight 587 given in Table I. Inserting a mean velocity of the small ions of $3 \times 10^4\ \frac{cm}{sec}$

we get

$$\frac{\sum \beta N}{\bar{v}} = 3 \times 10^{-8} \text{ cm}^2/\text{cm}^3$$

If all of the particles have a radius of 5.2×10^{-6} cm, the number density required is about 350 per cm^3. If the radius is increased by a factor of 10, the number density needed is only 3.5 per cm^3. Hence, contrary to the statement of Junge, Chagnon and Manson (1961), the ion density measurements are more than sufficiently sensitive to particulate matter. The concentrations of dust given by the ion density measurements are at least a factor of 20 higher than those given by Junge. In view of the uncertainties and inherent difficulties in the technique used by Junge, however, it is concluded that the ion density measurements are more representative of ambient conditions. It should be mentioned that the data point chosen for the calculation and comparison is typical.

The data shown in figures 16 and 18 are nearly identical to the profiles obtained for about 50% of the flights made since this program was initiated in 1958. However, there are cases where the nuclei content of the atmosphere is very high (figure 17). Before proceeding, the following question must be answered. If nuclei are so effective for removing small ions at high altitude where their number density is so low, then why are there any small ions in the troposphere where the nuclei count is high? The answer to this question is the following: At high pressures ($p > 150$ mb) the Thomson recombination coefficient (α) is as large as β for nuclei with $R \simeq r_o$. Hence, for the Aitken nuclei term to be important, the Aitken nuclei must exist in quantities comparable to the small ions. This is not the case since N is only about 200 per cm^3 in the troposphere. Furthermore, the larger nuclei ($R >> r_o$) are lost rapidly from the troposphere by washout, whereas the small nuclei ($R \simeq r_o$) require larger supersaturation in order for condensation to occur on them. On

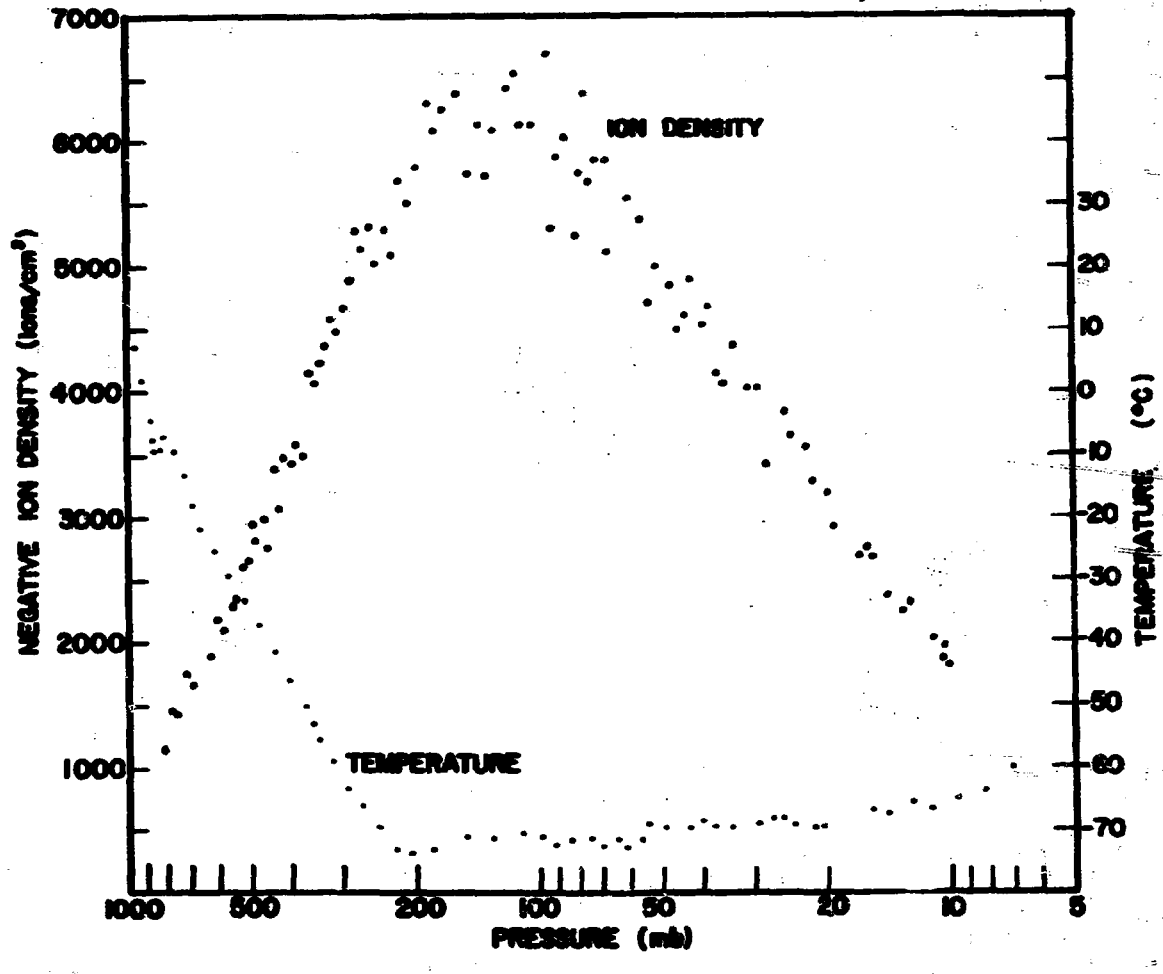

Fig. 18. The ion density and temperature profiles of flight 582 for April 19, 1962, over Minneapolis.

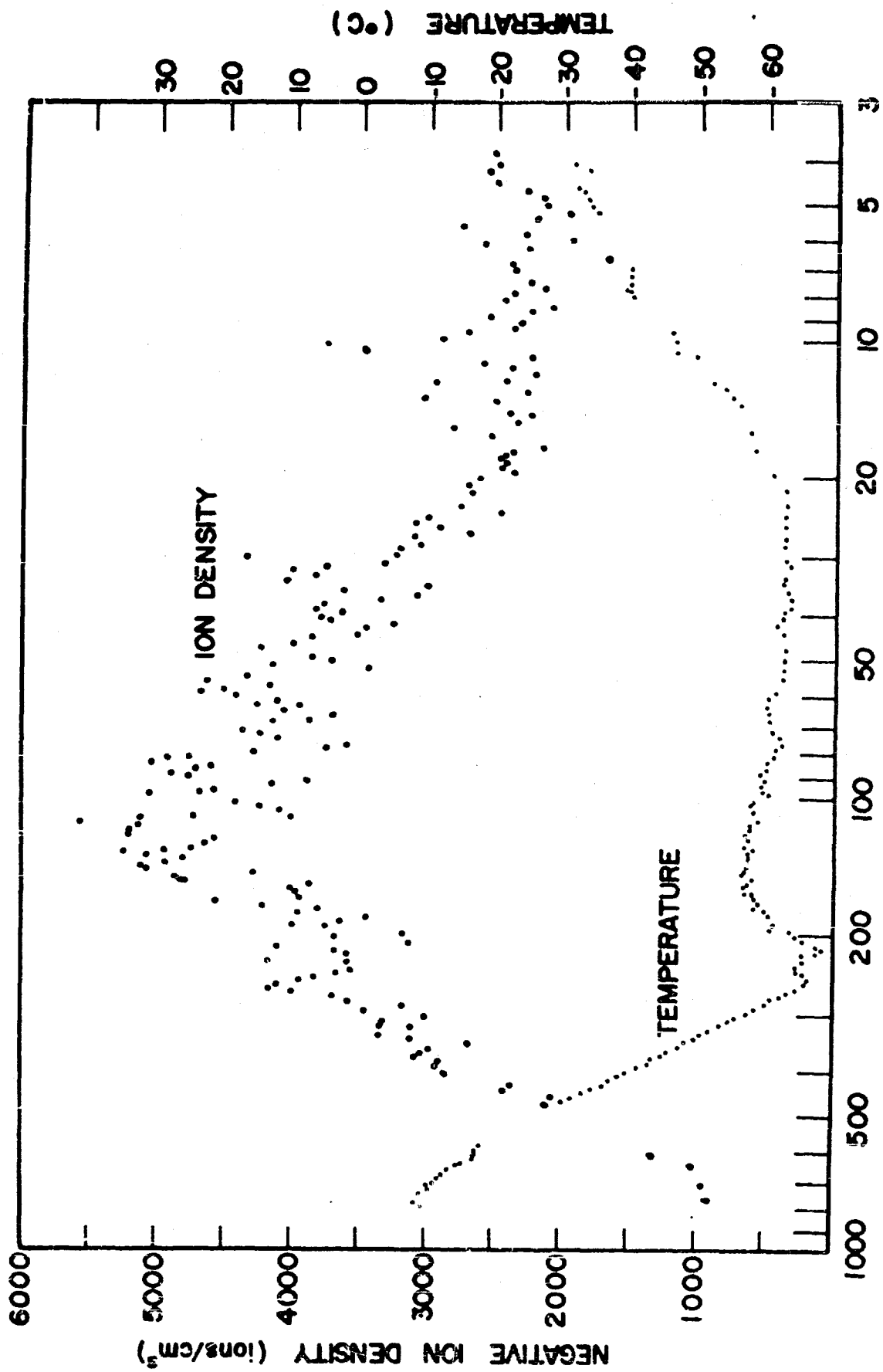

Fig. 19. The ion density and temperature profile of flight 527 for February 4, 1961, over Minneapolis.

occasion they should be present sufficient quantity, however, and this is born out by figure 17 and data presented elsewhere (Kroening, 1960). Moreover, at very low altitude in the troposphere, natural radioactive material is thrown up along with large nuclei, thus masking their presence.

The term $\Sigma \beta N/\bar{v}$ has another interesting aspect. Since this is the geometrical cross section of the particles per cm^3 if $R \geq r_o$, one might expect, on this basis, a variation in the atmospheric transparency. Zacharov (1952) indeed has found such a variation by analyzing the 10-year measurements of atmospheric transparency by Abbot and Fowle (1913) and has attributed it to particulate matter of a similar size and quantity suggested by the ion density measurements.

For example, if the nuclei are distributed more or less uniformly throughout an atmospheric scale height (10 km), we would estimate a total geometrical cross sectional area of .03 cm^2. Thus, an attenuation of 3% in the vertical would result. This assumes that the attenuation cross section is the same as the geometrical cross section. This is so for particles near the wavelength of light. Zacharov's attenuation factor was wavelength dependent as indicated below:

$\lambda(\mu)$	.35	.4	.45	.5	.6	.7	.8	1.0	1.2
$\frac{\Delta t}{t}$	.041	.035	.039	.026	.022	.015	.012	.0095	.0075

where t is the transparency of the atmosphere. From this selective attenuation, Zacharov concluded that the particles could not have diameters greater than 10^{-5} cm. Giovanelli (1954), on the other hand, using Zacharov's data concludes that the particles could have diameters larger than 10^{-5} cm. Giovanelli estimates the total number of particles to be

$\int N dz \approx 3 \times 10^6/cm^2$

He further assumes that they are distributed throughout a 10 km range and arrives at a number density of 3 particles per cm^3. This is, for practical purposes, the same as that required by the ion density measurements. It is concluded that the data of Junge, Chagnon and Manson (1961) are in error at these high altitudes. There are several critical points to be made regarding the data of Junge, Chagnon and Manson.

1. At the operating temperature of the expansion chamber (20°C) used to determine the nuclei count, the vapor pressure of water is 23.4 mb. This pressure corresponds to an altitude of 25 km in the atmosphere. From Junge's description of the apparatus, it is unclear as to how the measurements could be meaningful above 25 km. Prior to each expansion of the chamber 1000 cc of ambient air were supposedly drawn through the system within 20 seconds via an inlet and outlet valve. A pump was connected to the outlet. However, an experiment was performed by the author to determine the evaporation rate of water at this critical pressure (23.4 mb). In 25 seconds a 1 square inch wetted piece of black velvet at 20°C would evaporate 3500 cc of water vapor. From this one can only deduce that no fresh air entered the chamber and only that water vapor left both inlet and outlet valves the moment they were opened for sampling.

2. The efficiency of the detectors was calculated and not determined experimentally. This is just as serious as the previous criticism except that it applies at all altitudes.

3. No descent data were obtained since the equipment always failed at or before reaching ceiling altitude.

4. The statistics involved in some of the measurements was poor.

Now in regard to the ion density measurements there is only one known factor which could affect the results. That is the electrostatic effect of the

balloon. The magnitude of this effect is shown in figure 16 where both ascent and descent data are presented for the same flight. The variation between ascent and descent at 10 mb is a considerable factor and it is one of the largest observed. Moreover, it does not affect the above calculations sensibly. In all of the soundings the package is suspended 200 ft. below the balloon to minimize this effect.

Exception to the above statement is allowed for the two flights shown in figures 20 and 21. On these two flights and only on these two, there was the possibility that an electric field existed between the outside of the collector and the gondola. This external electric field would have the effect of reducing the collection rate of negative ions. These two flights are presented mainly for this purpose. Yet, there is the possibility that they do represent ambient conditions since the flights followed the Perseid and Arietid meteor showers. Furthermore, the sporadic meteor influx had already reached its maximum prior to these two flights.

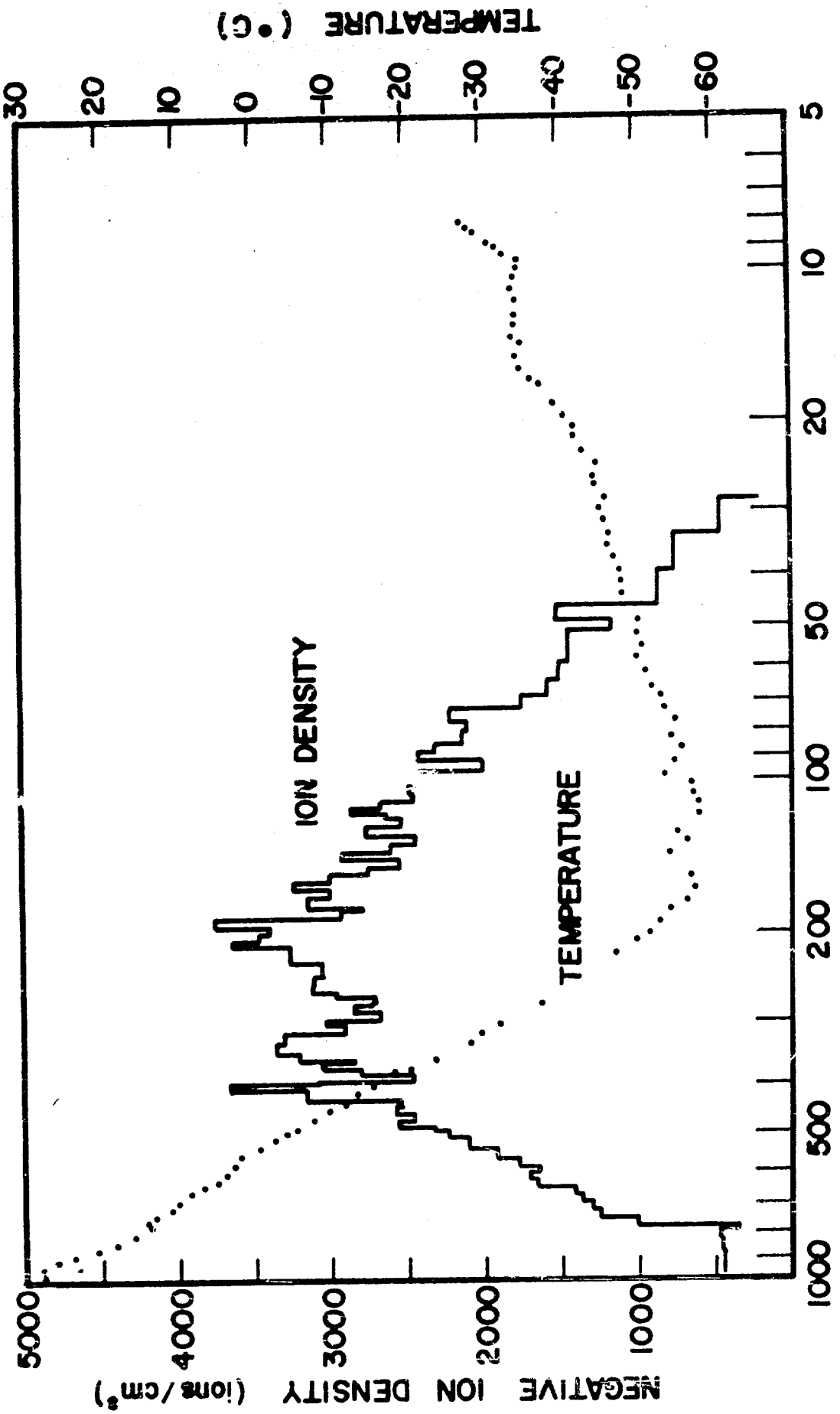

Fig. 20. The ion density and temperature profile of flight 602 for July 13, 1962, over Minneapolis.

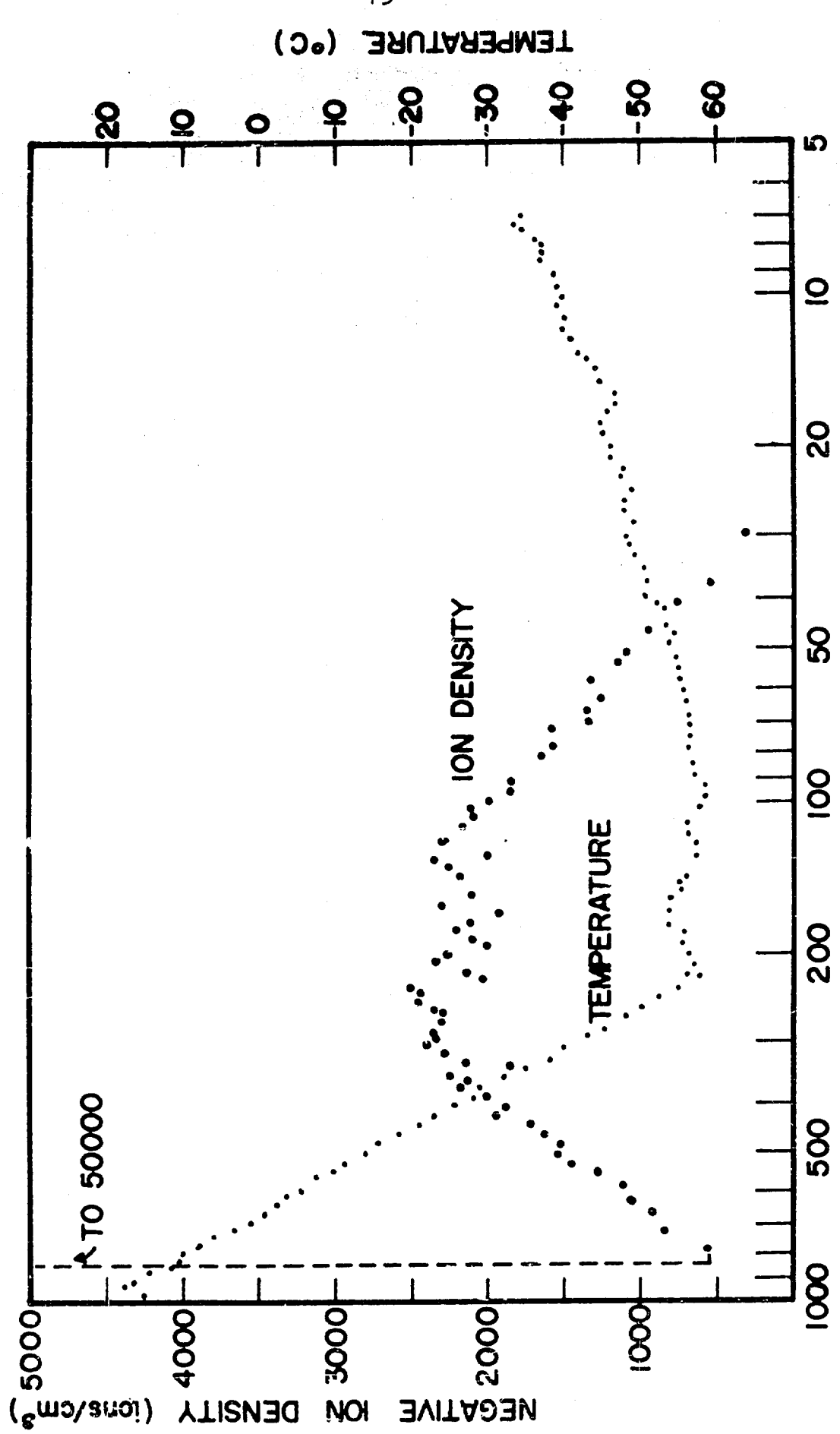

Fig. 21. The ion density and temperature profile of flight 603 for July 24, 1962, over Minneapolis.

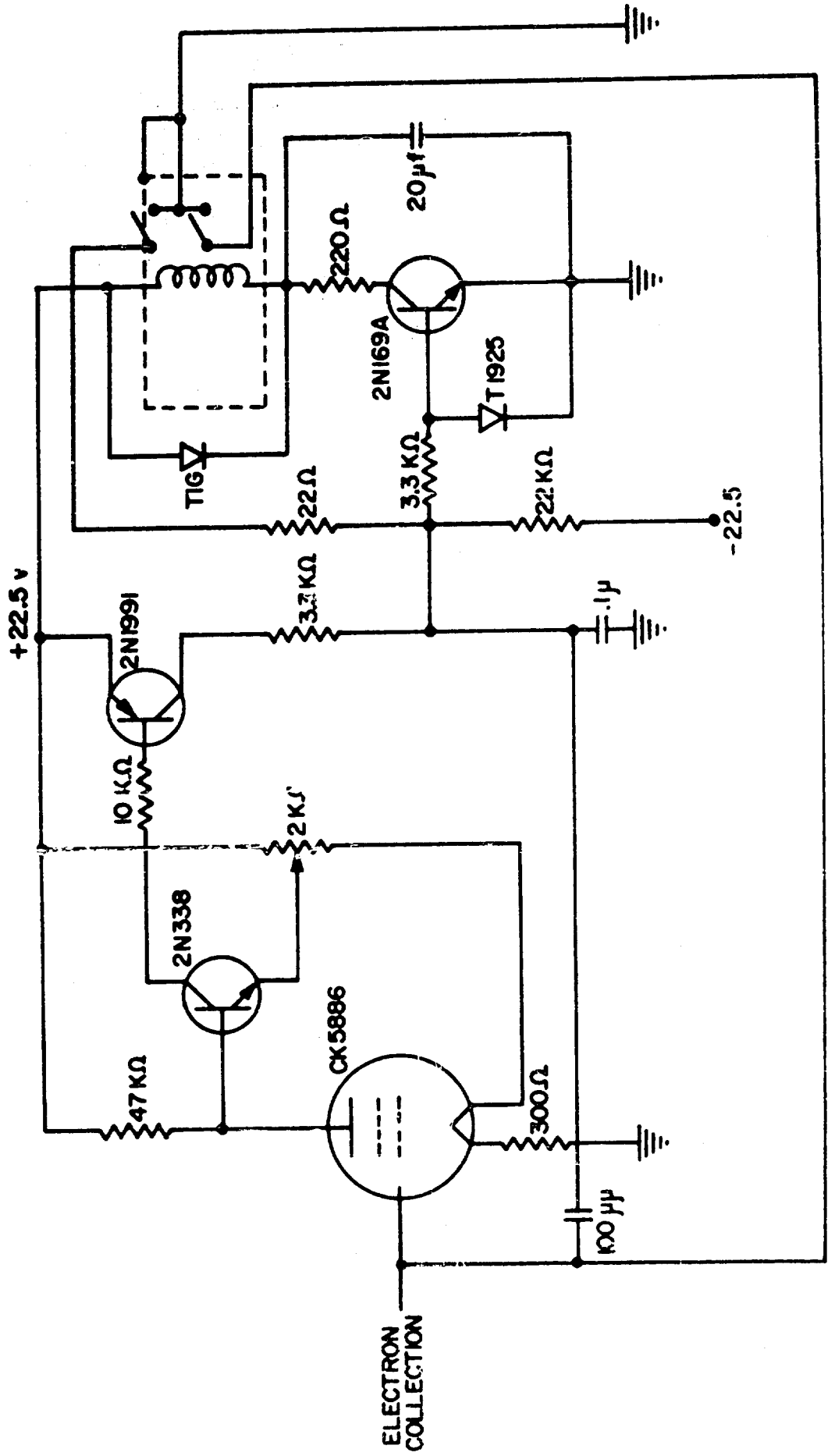

Fig. 22. Schematic diagram of the electrometer used in the ion density measurements.

ACKNOWLEDGEMENTS

The author is grateful to Professor Edward P. Ney for suggesting this work and for his invaluable assistance and encouragement through to its completion.

Special thanks go to Mr. Raymond Maas, not only for his numerous technical suggestions, but also for his untiring aid during most of this work. The author is thankful to Mr. James Stoddart and Mr. William Huch who likewise shared in the worry and work involved.

Many thanks are due to Mr. Robert Howard and the electronics shop staff, and to Mr. Rudolph Thorness and the machine shop group for their gratuitous technical assistance. Much of the instrument construction and data reduction was carefully done by Mr. James Rosen, Mr. Roger Marth and others whose help is greatly appreciated.

The author wishes to express his appreciation to the Office of Naval Research, who, under Contract Nonr-710(22), sponsored this research.

Finally, the author appreciates the many discussions with Professor Homer T. Mantis.

SMALL ION BIBLIOGRAPHY

Abbott, C.G., Fowle, F.E., and Aldrich, L.B., Ann. Astrophys., Obs. Smithson. Instr., Vol. 3 and 4, 1913.

Giovanelli, R.G., The Attenuation of light by metioric dust in the upper atmosphere. Australian J. of Phys., 7, pp. 641-648, 1954.

Junge, C.E., Chagnon, C.W., and Manson, J.E., Stratospheric Aerosols, J. of Meteorol., 18, pp. 81-108, 1961.

Kroening, J.L., Atmospheric Ionization, Master's Thesis, University of Minnesota, Minneapolis, Nov. 1959.

Ibid., Ion-density measurements in the stratosphere, J. of Geophys. Res., 65, pp. 145-157, 1960.

List, R.J., Radioactive tracers for stratospheric circulation, Arctic Meteorology Research Group, McGill University, Montreal, Publication in Metecrology, 47, 1962.

Machts, L. and List, R.J., Analysis of stratospheric strontium measurements, J. of Geophys. Res., 64, pp. 1269-1276, 1959.

Zacharov, I., Bull. Cent. Astr. Inst. Csl., 3, p. 82.